arXiv:1212.5414v1 [math.PR] 21 Dec 2012

ASYMPTOTIC DOMINO STATISTICS IN THE AZTEC DIAMOND

SUNIL CHHITA, KURT JOHANSSON, AND BENJAMIN YOUNG

Abstract. We study domino tilings on the Aztec diamond, with two different weights for horizontal and vertical dominos. Using a result of Helfgott, and a one-to-two lifting from the correlation kernel of a related interlaced particle system, we guess and then prove a formula for the inverse of the Kasteleyn matrix of the Aztec diamond. This lets us compute asymptotics for the determinantal *southern domino process*, using Kenyon's local statistics formula. We find that at the northern edge of the chaotic region, the southern domino process converge to a *thinned* version of the Airy point process. Conversely, at the southern edge of the chaotic region, the holes of the southern domino process converge to a *thickened* Airy point process, where one adds multiple points to the Airy point process. We also outline the proof that the fluctuations of the height function converge to the Gaussian free field.

1. Introduction

The *Aztec Diamond of order n* is a planar region which can be completely tiled with *dominos* — two-by-one rectangles. Over the past twenty years, this particular shape has come to occupy a central place in the literature of domino tilings of plane regions. Tilings of large Aztec diamonds exhibit striking features — the main one being that these tilings exhibit a limit shape, described by the so-called Arctic circle theorem [17]. The object of study in this paper is a perturbation of the uniform measure on domino tilings, in which vertical tiles are preferred over horizontal tiles. See Figure 1 for pictures of tilings of a relatively large Aztec diamond.

There are several alternate descriptions of a tiling of an Aztec diamond. A domino tiling is equivalent to a perfect matching, or *dimer cover*, on the dual graph of the region which is tiled. There is an equivalent family of nonintersecting lattice paths, called DR paths [32], and there is a description as a stack of a certain sort of blocks, called *Levitov blocks* [30, 31] (see Figure 1) There is also a well-studied *interlacing particle process* which is equivalent to the tiling model in a certain sense, but this equivalence is not bijective: there are $2^{n(n+1)/2}$ tilings of the Aztec diamond, whereas the number of configurations of the particle process are equinumerous with order-n *Alternating sign matrices* or configurations of the *six-vertex model*. However, the correspondence is *weight preserving* and *locally defined*; it maps certain

Key words and phrases. Aztec Diamond, dimer, domino, tiling, determinantal point processes, Gaussian Free field.

Department of Mathematics, Royal Institute of Technology (KTH), Stockholm, Sweden. E-mail: chhita@kth.se. The support of the Knut and Alice Wallenberg Foundation grant KAW:2010.0063 is gratefully acknowledged.

Department of Mathematics, Royal Institute of Technology (KTH), Stockholm, Sweden. E-mail: kurtj@kth.se. The support of the Swedish Research Council (VR) and the Knut and Alice Wallenberg Foundation grant KAW:2010.0063 are gratefully acknowledged.

Department of Mathematics, University of Oregon, Eugene, USA. Email: bjy@uoregon.edu. The support of the Knut and Alice Wallenberg Foundation grant KAW:2010.0063 is gratefully acknowledged.

collection of tilings to a configuration of the *free-fermion* six-vertex model [13], preserving the relative weights.

It is this point process whose local asymptotics have been studied most thoroughly [19]; in particular, the boundary of the frozen region is more easily described using the particles, since it is related to the position of the last particles on different lines. There is also a relationship between these particles and a certain sort of *zig-zag path* in the tiling (distinct from the zig-zag paths studied in [7]) which is helpful. However, the many-to-one nature of the correspondence necessarily loses some of the information about the original tilings. In both the domino and particle pictures, we get determinantal point processes, although the precise combinatorial relation between the two processes is not immediate.

We correct this situation in this paper, by giving a formula for the inverse Kasteleyn matrix for the Aztec diamond. This generalizes a previous result by Helfgott [16] to the case when the horizontal and vertical dominos have different weights. Using an observation of Kenyon [26], it is then possible to compute probabilities for various configurations of dominos and their asymptotic limits as the size of the Aztec diamond increases. In particular, we answer two questions about domino tilings of the Aztec diamond which would be much harder to state, or prove, in the interlaced particle process:

(1) How does the boundary of the frozen region manifest itself if we can only see one type of dominos, for example, the southern dominos?
(2) Do the fluctuations of the chaotic region of the Aztec diamond tend, as one would expect for any dimer model, to the Gaussian Free field?

1.1. **The southern domino process: North Boundary.** There are in fact four different types of dominos in a tiling: the dominos can be placed in two orientations, each of which comes in two different parities (determined by the bipartition of the dual graph on which the dominos are placed). Due to the Arctic circle theorem, with probability one, there are only dominos of one of these four types clustered near each of the four corners of the Aztec diamond. For this reason (and others, see [13]) we call the four types of dominos *north, south, east, and west*, which are coloured red, green, yellow and blue in Figure 1 in the electronic version of this article.

For the moment, ignore all but the south dominos (the green ones in Figure 1). Viewing each domino as a *point*, the set of all southern dominos form a determinantal point process. Note that the positions of the southern dominos do not specify the tiling uniquely so they only give a partial description of the tiling (though, together with any of the other types of dominos, they do). We analyze the distribution of the southern dominos along a diagonal line in a large Aztec diamond, scaled so as to study the two intersections between this line and the frozen boundary of the tiling (an "arctic ellipse", in the weighted case. It would be possible to extend what we have done to analyze the joint distribution of all southern dominos in the Aztec diamond; as is, our analysis extends previous results in [8] on placement probabilities of single dominos.

We will show that the appropriate scaling limit of the point process of southern dominos along a diagonal line close to the boundary of the *northern* frozen region is given by a thinned Airy kernel point process, where the amount of thinning depends on the relative weight of the horizontal and vertical dominos. This can be heuristically understood in the following way. The Airy kernel point process, as mentioned earlier, is the edge limit of the particle process along a diagonal line, and these in turn are given by the intersections of the non-intersecting paths and the diagonal line. Sometimes these intersections occur along a southern domino, and sometimes not. If we only see the southern dominos we only see some

of these intersections and which of them we see is essentially random; so we might expect, in the limit, a random thinning of the Airy kernel point process. *A priori* it is not clear that the thinning becomes independent in the limit, but this turns out to be the case.

1.2. **The southern domino process: South Boundary.** If, instead, we examine the southern frozen region, we find that almost all of the dominos are coming from the south domino process, and thus lie in a frozen, brickwork pattern predominantly. The southern boundary is a "hole" in this regular pattern. Consider the holes between the south dominos along a diagonal line in a neighborhood of the southern boundary. These holes also form a determinantal point process but in a scaling limit it does not converge to a *simple* process, but rather to a *multiple point process* with independent geometric probabilities for the points in an Airy kernel point process. This can be seen in Figure 1: there is a tendency for dominos of like types to cluster together along the southern boundary. This tendency continues even in the limit, with a cluster of k dominos becoming a point of multiplicity k. The multiplicity increases as we go towards the lower tangency point of the arctic ellipse, a fact which can also be observed in Figure 1.

We will also consider some scaling limits when the relative weight of vertical and horizontal dominos varies with n. Furthermore we will use our knowledge of the inverse Kasteleyn matrix to show the convergence of the height function to a Gaussian Free Field.

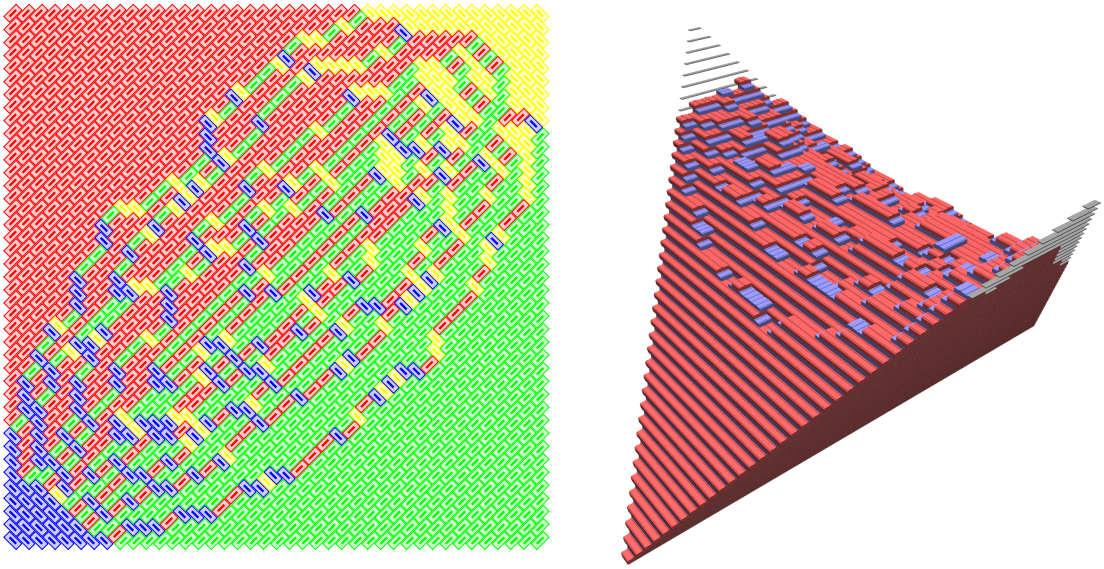
1.3. **Previous work.** Domino tilings on the Aztec diamond were originally introduced in [13] as a model connected with the *alternating sign matrices*. In this section, we give only a partial overview of the literature on the asymptotics of domino tilings of the Aztec diamond.

Due to the existence of limit shape of large tilings [8, 19], the Aztec diamond was one of the main motivating examples for the general theory of the existence of a limit shape for general tiling models on bipartite graphs [8, 9, 29]. For these particular tiling models, one can define a height function which is in bijection (up to height level) with the tiling [38]. The behavior in the bulk holds from the general results in [29] which says that the measure of domino tilings is locally a Gibbs measure and dependent on the average slope of the height function at the specified point.

The edge behavior, that is, the behavior between the frozen and unfrozen regions has, been of particular interest to the random matrix community, as the fluctuations are of size $n^{1/3}$. This is the same size as the fluctuations of the largest eigenvalue of the *Gaussian Unitary Ensemble (GUE)*. Indeed, [18, 19] showed that the law of the particles associated to the tiling is given by the *Airy process* and that the position of the last particle is given by the Tracy Widom distribution, F_2, see for example [1]. Furthermore, [21] showed that the distribution of these particles becomes the *GUE minor process* at the intersection of the liquid region and the boundary of the Aztec diamond while [14] obtained the similar results for a certain half Aztec diamond.

There are a handful of other explicitly inverted Kasteleyn matrices in the literature. The inverse of the Kasteleyn matrix of the Aztec diamond was computed by Helfgott [16] in the case of the uniform measure on domino tilings; the results in [9, 29] rely on explicit inverses of four Kasteleyn-like matrices that, together, count perfect matchings on a torus-embedded graph. Finally, Kasteleyn [22] computes the eigenvalues and eigenvectors of the Kasteleyn matrix of the $m \times n$ grid graph explicitly.

FIGURE 1. Left a tiling of an Aztec diamond with $a = \frac{1}{2}$, and the corresponding dimer cover. The green dominos along each horizontal row give the southern domino process. Right: the height function associated to this tiling (realized as a pile of Levitov blocks [30, 31]).



Acknowledgements. We would like to thank Alexei Borodin, Maurice Duits, Harald Helfgott, Richard Kenyon, Tony Metcalfe, Jim Propp, and David Wilson for enlightening conversations. We would like to thank MSRI (Berkeley) where part of this work was carried out and the Knut and Alice Wallenberg foundation for financial support, grant KAW2010.0063.

2. Preliminaries and Results

2.1. **Determinantal Process.** Determinantal point processes are a key part of the analysis used in this paper. Here, we briefly describe these processes but more in depth treatises of determinantal point processes can be found in [20] and [37].

Let Λ be a Polish space and take $\mathcal{M}(\Lambda)$ to denote space of counting measures ξ on E with $\xi(B) < \infty$ for every boundary $B \subset \Lambda$. A point process on Λ is a probability measure $\mathbb{P}$ on $\mathcal{M}(\Lambda)$. Let M_n denote the factorial moment measure, that is, for disjoint Borel sets $A_1, \dots, A_m$ in Λ,

$$M_n(A_1^{n_1} \times \cdots \times A_m^{n_m}) = \mathbb{E}\left[\prod_{i=1}^{m} \frac{\xi(A_i)!}{(\xi(A_i) - n_i)!}\right] \tag{2.1}$$

Suppose that λ is a reference measure on Λ. For example, if $\Lambda = \mathbb{R}$ we can choose λ to be the Lebesgue measure. If

$$M_n(A_1, \dots, A_n) = \int_{A_1 \times \cdots \times A_n} \rho_n(x_1, \dots, x_n) d\lambda(x_1) \dots d\lambda(x_n) \tag{2.2}$$

for all Borel sets A_i in Λ, we call ρ_n to be the n^{th} correlation function. For discrete processes, $\rho_n(x_1, \dots, x_n)$ is equal to the probability of seeing particles at $x_1, \dots x_n$, whereas for continuous processes, ρ_n is the density of seeing particles. For example, if $\rho_n(x_1, \dots, x_n) =$

$\rho(x_1)\dots\rho(x_n)$ where $\rho \in L^1$ with $\Lambda = \mathbb{R}$ and λ is the Lebesgue measure, then the point process is the Poisson point process on $\mathbb{R}$.

A point process is called *determinantal* if there exists a function $\mathbb{K} : \Lambda \times \Lambda \to \mathbb{C}$ called the correlation kernel, with

$$\rho_n(x_1, \dots, x_n) = \det\left(\mathbb{K}(x_i, x_j)\right)_{i,j=1}^n. \tag{2.3}$$

This leads to the following characterization of a determinantal point process. Let $C_c^+(\Lambda)$ be the set of all non-negative continuous functions on Λ with compact support. Take $\psi \in C_c^+(\Lambda)$, let A denote the support of ψ and set $\phi = 1 - e^{-\psi}$. Let 1_A denote the indicator function for the set A. Then, provided $\phi K 1_A$ is trace class and the Fredholm determinant is given by its Fredholm expansion,

$$\mathbb{E}\left[e^{-\sum_j \psi(x_j)}\right] = \det(I - \phi K 1_A)_{L^2(\Lambda,\lambda)}, \tag{2.4}$$

where x_j are the points in the process.

2.2. **Kasteleyn Matrix for the Aztec Diamond.** For a bipartite graph, the Kasteleyn matrix, introduced in [23] to count perfect matchings of a graph, is a signed weighted (possibly complex entried) adjacency matrix with rows indexed by the black vertices and columns indexed by the black vertices. We describe the Kasteleyn matrix for the Aztec diamond below but first remind the reader of two theorems.

Suppose that K denotes the Kasteleyn matrix for a finite bipartite graph G.

Theorem 2.1 ([23])**.** *The number of weighted dimer coverings of G is equal to $|\det K|$*

Suppose that $E = \{e_i\}_{i=1}^n$ are a collection of distinct edges with $e_i = (b_i, w_i)$, where b_i and w_i denote black and white vertices.

Theorem 2.2. *The dimers form a determinantal point process on the edges of G with correlation kernel given by*

$$L(e_i, e_j) = K(b_i, w_i)K^{-1}(w_j, b_i) \tag{2.5}$$

where $K(b, w) = K_{bw}$ and $K^{-1}(w, b) = (K^{-1})_{wb}$

Proof. By [24], we have that the probability of finding dimers at the edges $e_1, \dots, e_n$ is

$$\begin{aligned}\mathbb{P}(e_1, \dots, e_n) &= \prod_{i=1}^n K(b_i, w_i) \det\left(K^{-1}(w_j, b_i)\right)_{i,j=1}^n \\ &= \det\left(K(b_i, w_i)K^{-1}(w_j, b_i)\right)_{i,j=1}^n \\ &= \det\left(L(e_i, e_j)\right)_{i,j=1}^n\end{aligned} \tag{2.6}$$

□

An Aztec diamond of size n is a region of lattice squares described by $\{(x, y) : |x| + |y| \leq n + 1\}$. A domino is a two by one rectangle that can be placed vertically or horizontally on the Aztec diamond. A domino tiling of the Aztec diamond is a covering of the Aztec diamond so that each square is covered exactly once by a domino. An equivalent viewpoint is to replace the Aztec diamond by its dual graph and a domino replaced by a dimer which is an edge. We rotate the Aztec diamond by $\pi/4$ counter clockwise. As the Aztec diamond, its dual graph, a domino and a dimer are synonymous, we will interchange between the definitions. Figure 2 shows the rotated Aztec diamond and a dimer covering of the dual graph.

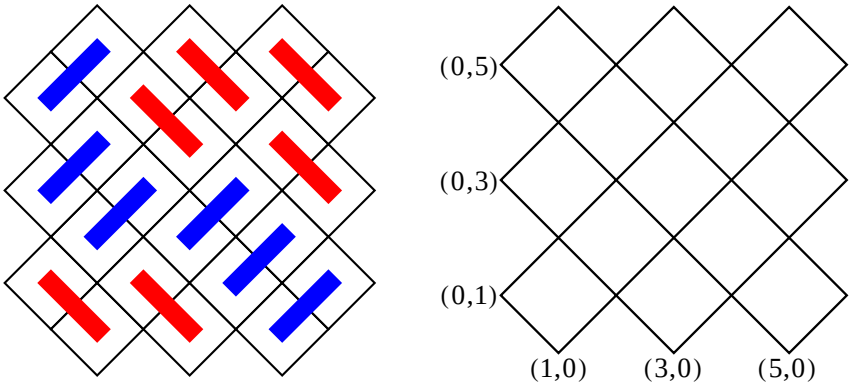


FIGURE 2. The figure on the left shows an Aztec diamond of size 3 with a dimer covering of the dual graph. The domino tiling can be seen by placing dominos over the dimers. The figure on the right shows the co-ordinates of the Aztec diamond (dual graph) – the whtie vertices $x = (x_1, x_2)$ have $x_1 \mod 2 = 1$ and $x_2 \mod 2 = 0$ while the black vertices are the remaining vertices.

We give the (dual graph) Aztec diamond of size n the following co-ordinates: let $\mathtt{W}$ and $\mathtt{B}$ denote the set of white and black vertices for an Aztec diamond of size n. We have that

$$\mathtt{W} = \{(x_1, x_2) : x_1 \in 2\mathbb{Z} + 1, x_2 \in 2\mathbb{Z}, 1 \leq x_1 \leq 2n - 1, 0 \leq x_2 \leq 2n\} \tag{2.7}$$

and

$$\mathtt{B} = \{(y_1, y_2) : y_1 \in 2\mathbb{Z}, y_2 \in 2\mathbb{Z} + 1, 0 \leq y_1 \leq 2n, 1 \leq y_2 \leq 2n - 1\}. \tag{2.8}$$

Set $e_1 = (1, 1)$ and $e_2 = (-1, 1)$. We have that $x \in \mathtt{W}$ is adjacent to $y \in \mathtt{B}$ iff $y - x = \pm e_i$ for $i \in \{1, 2\}$. See Figure 2 for the co-ordinates of an Aztec diamond of size 3.

For $w \in \mathtt{W}$ and $b \in \mathtt{B}$, a dimer (w, b) is labeled *horizontal* if $|w - b| = e_1$ and is labeled vertical if $|w - b| = e_2$. A dimer is labeled *north* (respectively *south*) if it is a horizontal edge with a black leftmost (resp. rightmost) vertex. A dimer is labeled *east* (respectively *west*) if it is vertical edge with a black leftmost (resp. rightmost) vertex.

We are free to choose any Kasteleyn orientation and so we choose the same Kasteleyn orientation used in [26] which is given by the following: for notational purposes, let

$$\mathtt{W}_i = \{(x_1, x_2) \in \mathtt{W} : (x_1 + x_2) \mod 4 = 2i + 1\}, \tag{2.9}$$

and

$$\mathtt{B}_i = \{(y_1, y_2) \in \mathtt{W} : (y_1 + y_2) \mod 4 = 2i + 1\}. \tag{2.10}$$

for $i \in \{0, 1\}$. The edges incident to each vertex in $\mathtt{W}_0$ have edge weights $-ia, -1, ia, 1$ with the labeling given by proceeding clockwise from the edge leaving the white vertex in the direction of e_2. The edges incident to each vertex in $\mathtt{W}_1$ have edge weights $ia, 1, -ia, -1$ with the labeling given by proceeding clockwise from the edge leaving the white vertex in the direction of e_2. These weights are depicted in Figure 3.

Let A_n denote the vertices given in the above co-ordinates with side length $2n$. Let $\partial_l A_n$ denote the vertices in $A_n \cap \mathtt{B}$ of the form $(0, 2k - 1)$ and $\partial_r A_n$ denote the vertices in $A_n \cap \mathtt{B}$ of the form $(2n, 2k - 1)$ for $1 \leq k \leq n$.

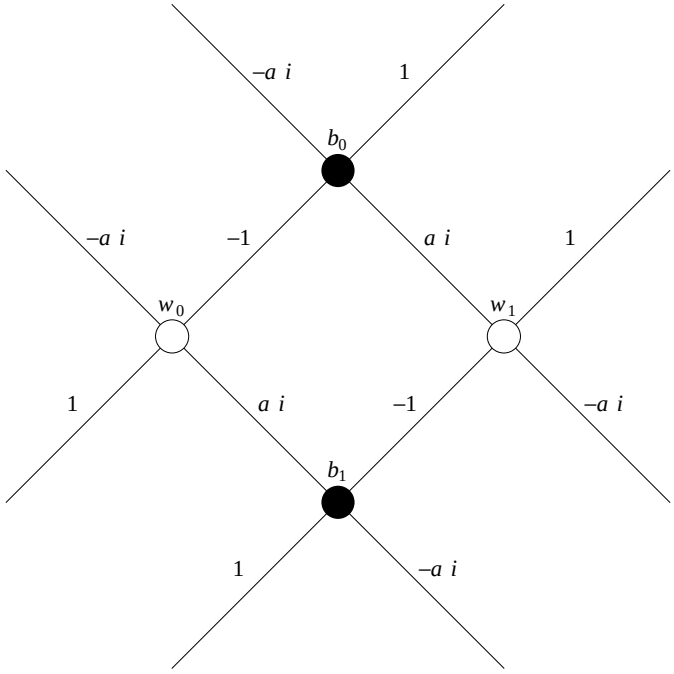


FIGURE 3. The complex weights with $w_i \in \mathtt{W}_i$ and $b_j \in \mathtt{B}_j$.

For the rest of the paper, let K denote the Kasteleyn matrix for A_n with the above weights, that is, $K : \mathtt{B} \times \mathtt{W} \to \mathbb{C}$ where $K(b, w) = K_{b,w}$ for $b \in A_n \cap \mathtt{B}$ and $w \in A_n \cap \mathtt{W}$ with

$$K(b,w) = \begin{cases} (-1)^{l+j} & \text{if } b \in \mathtt{B}_j, w = b + (-1)^l e_1, b \notin \partial_r A_n, l \in \{0,1\} \\ (-1)^{l+j} ai & \text{if } b \in \mathtt{B}_j, w = b - (-1)^l e_2, b \notin \partial_l A_n, l \in \{0,1\} \\ 0 & \text{otherwise.} \end{cases} \tag{2.11}$$

We can define the Kasteleyn operator $K : \mathbb{C}^{\mathtt{B}} \to \mathbb{C}^{\mathtt{W}}$ for $v \in \mathtt{B}$ and for $f : \mathtt{B} \to \mathbb{R}$

$$Kf(v) = \sum_{w \sim v} K(w,u) f(v) \tag{2.12}$$

where $w \sim v$ means nearest neighbors. As A_n is finite, we shall interchange between operators and matrices without further mention.

2.3. **Height Function.** The height function is defined on the faces of the square grid and is defined as follows: the height change between two adjacent faces is ± 3 if there is a dimer covering the shared edge between the two faces and ∓ 1 otherwise. As we traverse between two adjacent faces, we choose the sign convention to be $+3$(or respectively -3) if the left vertex is white (or respectively) black. The definition is consistent around each vertex, that is, the total height change around each vertex is zero. The dimer model is in bijection with the difference of heights between the faces of the graph.

We denote the height function of the Aztec diamond by h_n which is given by the following: the height change along the diagonal faces adjacent to the boundary of the Aztec diamond is ± 2. Suppose that the height function at $(0, 0)$ is 0, then the height function at both $(2r, 0)$ and $(0, 2r)$ is equal to $-2r$ for $1 \le r \le n-1$ while the height function at both $(2n, 2r)$ and

$(2r, 2n)$ is equal to $2r - 2n$ for $0 \leq r \leq n$. For a face f in the Aztec diamond, we have

$$h_n(f) = \sum_{i=0}^{m-1} (-1)^{\gamma[i]}(3X_{\gamma[i]} - 1) \tag{2.13}$$

where γ is a fixed path from $(0,0)$ to f of length m, $\gamma[i]$ is the i^{th} index of the path and $X_{\gamma[i]}$ is the indicator function that a dimer is traversed from $\gamma[i]$ to $\gamma[i+1]$. Figure 1 shows a realization of the height function for a random tiling of the Aztec diamond.

2.4. **Asymptotic Coordinates, average height function and the arctic ellipse.** In this subsection, we introduce the coordinates of frozen region as well as the average height function and the southern domino process. As $n \to \infty$, for the (re-scaled) Aztec diamond with corners $(0,0), (1,0), (0,1)$ and $(1,1)$, the boundary between the frozen and unfrozen regions is an ellipse [8] whose equation is given by

$$\frac{(v-u)^2}{1-p} + \frac{(u+v-1)^2}{p} = 1 \tag{2.14}$$

where $u \in [0,1]$ is the horizontal coordinate, $v \in [0,1]$ is the vertical coordinate, and $p = 1/(1+a^2)$. We let $\mathcal{D} \subset \mathbb{R}^2$ be the area bounded by the ellipse given in (2.14).

The average height function was computed in [8] for $a = 1$ and can be extended for all values of a. From [8], define

$$P(x, y, p) = \frac{1}{2} + \frac{1}{\pi} \arctan \frac{y - (1-p)}{\sqrt{p - p^2 - (1-p)x^2 - py^2}} \tag{2.15}$$

which is the asymptotic placement probability of a north domino on an Aztec diamond with corners $(1,0), (0,1), (-1,0)$ and $(0,-1)$. The asymptotic placement probabilities of south, east and west dominos are given by $P(-x,-y,p)$, $P(-y,x,1-p)$ and $P(y,x,1-p)$ respectively. Let

$$\overline{h}_r(x,y) = 2(yP(x,y,p) - yP(-x,-y,p) + (1-x)P(-y,x,1-p) + (1+x)P(y,-x,1-p). \tag{2.16}$$

The asymptotic height function for an Aztec diamond with co-ordinates $(0,0), (1,0), (0,1)$ and $(1,1)$ is given by

$$\overline{h}(u,v) = \overline{h}_r((1+u+v)/2, (1+u-v)/2) \tag{2.17}$$

which can be checked by showing it verifies the two differential equations obtained from the expected heights across a face and its boundary conditions.

We remark that $\frac{\partial}{\partial u}\frac{\partial}{\partial v}\overline{h}(u,v)$ is equal to the so-called *Archimedes measure* [2], which is the conjectured measure of the asymptotic density of 1's of the permutation matrix of a random sorting network. More details on random sorting networks can be found in [2].

The boundary of the arctic ellipse is given by

$$v = 1 - u \pm 2\sqrt{(1-p)p(1-u)u} + p(2u-1). \tag{2.18}$$

The arctic ellipse can be parametrized by $(u(k), v(k))$, where $v(k) = 1 - k^2 u(k)$ and

$$u(k) = \frac{1}{(1+a^2)(1+k^2) + 2a\sqrt{1+a^2}k}. \tag{2.19}$$

We will be interested in two parts of the boundary. The part where $k > 0$ will be called the *northern boundary* and the part where $k \in (-a^{-1}(1+a^2)^{1/2}, -a(1+a^2)^{-1/2}) = (-1/\sqrt{1-p}, -\sqrt{1-p})$ the *southern boundary*.

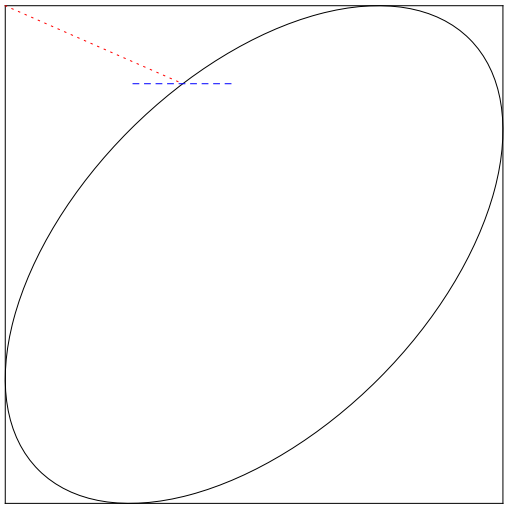


FIGURE 4. This figure shows the intersection of the limiting ellipse with the red dotted line given by $v = 1 - k^2 u$. The south dominos on the blue dashed line represent the southern domino process. The northern boundary lies between A and B and the southern boundary between C and D

See Figure 4 for an example of the northern and southern boundary and an explanation of the geometric meaning of k.

2.5. **Local Gibbs Measure.** In this subsection, we briefly describe the local Gibbs measures for the dimer model but a more formal account can be found in [29] and [28]. For all doubly periodic bipartite weighted dimer models embedded on the plane, [29] found that the dimer model is a Gibbs measure and also gave an explicit method to compute the entries of the inverse Kasteleyn matrix embedded in the plane. The results from [29] rely on using the smallest non-repeating of the graph unit called the *fundamental domain*. For the graph considered in this paper, the fundamental domain has one black vertex and one white vertex. In order to describe the Gibbs measure, [29] introduced magnetic co-ordinates (B_x, B_y) where one increases the energy by e^{B_x} or e^{B_y} if one crosses to the neighboring fundamental domain to the left or above. Conversely, if one crosses to the fundamental domain to the right or below, one decreases the energy by e^{B_x} or e^{B_y}. These magnetic co-ordinates are related to the average slope, that is, one can compute the Gibbs measures for different slopes, see [29].

We choose the fundamental domain of the graph in this paper (embedded on the plane) to be given by a white vertex, an edge parallel to e_2 which has weight ai and its incident black vertex. The edges parallel to e_1 are given weight 1. This choice of weighting is the same as the choice of weighting in Section 2.2 up to Kasteleyn orientation. We denote the Gibbs measure of the model on this graph by $\mu_a(B_x, B_y)$ where (B_x, B_y) is described above. Suppose that $(2\xi_1 + 1, 2\xi_2)$ is a white vertex and $(2\eta_1, 2\eta_2 + 1)$ is a black vertex for $\eta_1, \eta_2, \xi_1, \xi_2 \in \mathbb{Z}$. Suppose that (B_x, B_y) are the magnetic co-ordinates as described above. Using techniques from [29] one can find the entries of the inverse of the (infinite) Kasteleyn matrix, denoted by K_μ^{-1} and they are given by

$$K_\mu^{-1}((2\xi_1 + 1, 2\xi_2), (2\eta_1, 2\eta_2 + 1)) = \frac{1}{(2\pi i)^2} \int_{|z|=1} \int_{|w|=1} \frac{z^{\eta_1 - \xi_1} w^{\eta_2 - \xi_2}}{P(ze^{B_x}, we^{B_y})} \frac{dw}{w} \frac{dz}{z} \tag{2.20}$$

where $P(z,w)$ is the so-called *characteristic polynomial* defined in [29] and is given by

$$P(z,w) = ai + z^{-1} + w^{-1} + aiw^{-1}z^{-1}. \tag{2.21}$$

One consequence of knowing (2.20) is that by using Theorem 2.2, we can compute the probability of any cylinder set.

2.6. **Gaussian Free Field.** Another consequence of finding the inverse Kasteleyn matrix for domino tilings on the Aztec diamond and its corresponding asymptotics is that we are able to show that the fluctuations of the height function in the liquid region are governed by the Gaussian Free Field in the limit. This subsection introduces the Gaussian Free Field but a more in depth treatise can be found in [36].

The Gaussian Free Field F on $\mathbb{H}$ is a probability measure on the set generalized functions on $\mathbb{H}$ such that for any compactly supported test functions ϕ_1, ϕ_2, $\langle F, \phi_1\rangle := \int_{\mathbb{H}} F(z)\phi_1(z)|dz|^2$ is a real Gaussian random variable with mean zero and variance

$$\mathbb{E}[\langle F,\phi_1\rangle \langle F,\phi_2\rangle] = \int_{\mathbb{H}^2} \phi_1(z_1)\phi_2(z_2)G(z_1,z_2)|dz_1|^2|dz_2|^2 \tag{2.22}$$

where

$$G(z_1,z_2) = -\frac{1}{2\pi}\log\left|\frac{z_1-z_2}{z_1-\overline{z_2}}\right|. \tag{2.23}$$

For any finite sequence of compactly supported test functions $\{\phi_k\}$, the Gaussian Free Field F on $\mathbb{H}$ can be uniquely characterized [25] by its variance and that we can write

$$\mathbb{E}[\prod_{k=1}^{m}\langle \phi_k, F\rangle] = \begin{cases} 0 & m \text{ is odd} \\ \sum_{\text{pairings}} \mathbb{E}[\langle F,\phi_{\sigma(1)}\rangle \langle F,\phi_{\sigma(2)}\rangle]\dots\mathbb{E}[\langle F,\phi_{\sigma(m-1)}\rangle \langle F,\phi_{\sigma(m)}\rangle] & m \text{ is even.}\end{cases} \tag{2.24}$$

where the sum is over all $(2m-1)!!$ pairings

2.7. **Statement of Results.** Let $c : \mathtt{W}\times\mathtt{B}\to\mathbb{R}$ denote the coupling function, that is $C = K^{-1}$. The coupling function was originally computed in [16] for the uniform measure, by an explicit enumeration of a signed counting of domino tilings — the information encoded by the inverse Kasteleyn matrix. We generalize the coupling function so that we can consider different weights for vertical and horizontal tiles using the following method: By using the interlaced particle system [18, 19], we guess the entries of the inverse Kasteleyn matrix and show that the guess is correct. We remark that the correlation from the interlaced particle system and the correlations kernel from the inverse Kasteleyn matrix are not in bijection for domino tilings of the Aztec diamond which differs to the lozenge tiling model [34]. We obtain

Theorem 2.3. *For $x=(x_1,x_2)\in\mathtt{W}$ and $y=(y_1,y_2)\in\mathtt{B}$ we have*

$$c(x,y) = \begin{cases} f_1(x,y) & \text{for } x_1 < y_1+1 \\ f_1(x,y) - f_2(x,y) & \text{for } x_1 \geq y_1+1\end{cases} \tag{2.25}$$

where

$$f_1(x,y) = \frac{(-1)^{(y_1+y_2+x_1+x_2)/4}}{(2\pi i)^2}\int_{\mathcal{E}_2}\int_{\mathcal{E}_1} \tag{2.26}$$

$$\frac{w^{y_1/2}}{z^{(x_1+1)/2}(w-z)}\frac{(a+z)^{x_2/2}(az-1)^{(2n-x_2)/2}}{(aw-1)^{(2n+1-y_2)/2}(a+w)^{(y_2+1)/2}}dz\,dw \tag{2.27}$$

and

$$f_2(x,y) = \frac{(-1)^{(x_1+x_2+y_1+y_2)/4}}{2\pi i} a^{(y_2-x_2-1)/2} \int_{\mathcal{E}_1} \frac{z^{(y_2-x_2-1)/2}(1/a+z)^{(y_1-x_1-1)/2}}{(1/a+a+z)^{(y_2-x_2+1)/2}} dz \tag{2.28}$$

where $\mathcal{E}_1$ is the positively oriented contour $|z| = \epsilon$, $\mathcal{E}_2$ is the positively oriented contour $|w - 1/a| = \epsilon$ and the contours do not intersect.

The original approach for computing asymptotic quantities for domino tilings on the Aztec diamond used a non-intersecting particle system [18, 19] adapted from the so-called DR lattice paths [32]. Although much insight and information is gathered from this approach, the method does not allow one to compute the local statistics of the underlying dominos exactly.

For the proof of Theorem 2.3, we have a set of relations that the inverse of the Kasteleyn matrix should satisfy from the relation $K.K^{-1} = \mathbb{I}$. Indeed a similar set of relations (without a boundary condition) was used in [4], where the authors show that the correlation kernels of a family of interlaced particle systems satisfy the Gibbs property in the bulk.

Using Theorems 2.2 and 2.3, we can now compute all local statistics of the dominos, in particular, we compute all local statistics of the southern domino process which is defined as follows: fix r, $1 \leq r \leq n$. With a south domino on the line $y = r$ we mean a domino with a white vertex $w = (2x-1, 2r)$ and a black vertex $b = (2x, 2r+1)$ for some $x \in \{1, \ldots, n\}$, and we say that the south domino is located at x on the line $y = r$. The south dominos form a determinantal process by Theorem 2.2 and in particular so do the south dominos on the line $y = r$ with the kernel given by the following lemma:

Lemma 2.4. *The kernel of the determinantal process given by the positions of the southbound dominos on a fixed line $y = r$ in a random tiling of an Aztec diamond is*

$$L(x_1, x_2) := -\frac{1}{(2\pi i)^2} \int_{\mathcal{E}_1} \int_{\mathcal{E}_2} \frac{w^{x_2}}{z^{x_1}} \frac{(a+z)^r (az-1)^{n-r}}{(aw-1)^{n-r}(a+w)^{r+1}(w-z)} dw\, dz \tag{2.29}$$

Proof. Theorem 2.3 gives the coupling function as $c_1(w,b) = f_1(w,b) - f_2(w,b)$, but in this case

$$f_2(w,b) = \frac{(-1)^{\frac{x+y}{2}+r}}{2\pi i} \int_{|z|=\epsilon} \frac{(1/a+z)^{y-x-1}}{1/a+a+z} dz = 0 \tag{2.30}$$

because the integrand is analytic at $z = 0$. The result now follows by applying Theorem 2.2. The sign in front of the kernel will be $-(-1)^{(x_2-x_1)/2}$ and we can remove the factor $(-1)^{(x_2-x_1)/2}$ by a conjugation. □

Consider a determinantal point process ν on a space Λ with correlation kernel K. Let $0 \leq \alpha \leq 1$ and consider the point process obtained by removing each point in the process independently with probability $1 - \alpha$. We will call this new point process the *thinned determinantal point process* with correlation kernel K and parameter α. A way of modifying the original point process to obtain a point process with multiple points is by taking each point in the process ν independently with multiplicity m, where m is a geometric random variable with parameter β, $\mathbb{P}[m = k] = (1-\beta)\beta^{k-1}$, $k \geq 1$. We will call this (multiple) point process a *thickened determinantal point process* with correlation kernel K and parameter β.

Propostion 2.5. *The thinned determinantal point process $\{x_j\}$ with correlation kernel K and parameter α is again a determinantal point process with correlation kernel αK, i.e.*

$$\mathbb{E}\left[e^{-\sum_j \psi(x_j)}\right] = \det(I - \phi\alpha K 1_A), \tag{2.31}$$

for every $\psi \in C_c^+(\Lambda)$, $\phi = 1 - e^{-\psi}$ and $A = supp\,\psi = supp\,\phi$. With the same notation the thickened determinantal point process with kernel K and parameter β is characterized by

$$\mathbb{E}\left[e^{-\sum_j \psi(x_j)}\right] = \det\left(I - \frac{\phi}{1-\beta-\beta\phi} K 1_A\right), \tag{2.32}$$

where $\{x_j\}$ is now the multi-set of points of the process.

We will prove the proposition in Section 4. Note that the thickened process is no longer a determinantal point process since they are always simple point processes.

We will now consider the southern domino process along the northern and southern boundaries. Along the southern boundary the southern domino process is almost dense and we have to consider the dual process, the process of holes, instead. If we think of the locations in $1, \dots, n$ of the southern dominos on the line $y = r$ as positions of particles then the empty spaces, the holes, also form a determinantal point process with a kernel $I - L$, where L is the kernel for the particles.

In our scaling limits we will obtain the *Airy kernel point process* which is a determinantal point process with kernel

$$K_{Ai}(x,y) = \int_0^\infty \mathrm{Ai}(x+t)\mathrm{Ai}(y+t)dt. \tag{2.33}$$

Set

$$\beta = -a(a + k\sqrt{1+a^2}), \tag{2.34}$$

$$\alpha = \frac{1}{1-\beta} = \frac{1}{1 + a^2 + ak\sqrt{1+a^2}}, \tag{2.35}$$

and let $\lambda > 0$ be given by

$$\lambda^3 = \pm \frac{a(a + k\sqrt{1+a^2})^2}{(1+a^2)(ak^2 + k\sqrt{1+a^2})((1+a^2)(1+k^2) + 2ak\sqrt{1+a^2})} \tag{2.36}$$

with the plus sign for $k > 0$ and the minus sign for $k < 0$.

Theorem 2.6. *Let $a > 0$ be fixed let λ be given by (2.36), α by (2.35) and β by (2.34). Furthermore, let $\{x_j\}$ be the positions of the south dominos on the line $y = [(1 - k^2 u(k)n]$, where $u(k)$ is given by (2.19). Consider a fixed $k > 0$. Then, the rescaled south domino process at the northern boundary,*

$$\xi_j = \frac{nu(k) - x_j}{\lambda n^{1/3}}$$

converges to the thinned Airy kernel point process with parameter α.

Next, consider a fixed $k \in (-a^{-1}(1+a^2)^{1/2}, -a(1+a^2)^{-1/2})$. Let $\{y_j\}$ be the positions of the holes in the south domino process, i.e. the dual south domino process, at the southern boundary. The rescaled point process

$$\xi_j = \frac{y_j - nu(k)}{\lambda n^{1/3}}$$

converges weakly to the thickened Airy kernel point process with parameter β.

Successive independent thinning and rescaling of a point process typically has a Poisson point process as its limit. If a tends to infinity, we see that the thinning parameter of the thinned Airy kernel α tends to zero. Hence we can expect that if we let a tend to infinity

with n (but not too fast) the south domino point process close to the northern boundary should converge to a Poisson process. This leads to the next theorem.

Theorem 2.7. *Fix $k > 0$ and let $a = a(n)$, where $a(n) \to \infty$ but $a(n)/n^{1/10} \to 0$ as $n \to \infty$. Set $c(a) = \pi^{2/3}(1 + 1/k)^{1/3}a^{2/3}$ and let $\{x_j\}$ be the positions of the south dominos on the line $y = [n(1 - k^2u(k))]$. Then the rescaled point process*

$$\xi_j = \frac{nu(k) + c(a)n^{1/3} - x_j}{c(a)n^{1/3}} \tag{2.37}$$

converges weakly to a Poisson process with density $\rho(\xi) = \sqrt{(1-\xi)_+}$.

The condition on the allowed growth of $a(n)$ is certainly not optimal but is an outcome of the proof. A similar result holds for the thinned Airy kernel point process on $\mathbb{R}$: if the thinning parameter is sent to zero, the Airy kernel can be re-scaled to a Poisson point process on $\mathbb{R}$ which has a square root drop off. This result actually follows from the proof of Theorem 2.7. Thus, we can think of the thinned Airy kernel point process as being an intermediate kernel between the Airy kernel and the Poisson point processes. We could also consider the behaviour of the leftmost south domino along the northern boundary. For a fixed a we will get convergence to the last particle distribution for the thinned Airy kernel point process, $\det(I - \alpha K_{\text{Airy}})_{L^2(\xi,\infty)}$. When a goes to infinity with n but not too fast we will instead get one of the classical extreme value distributions in the limit, namely the last particle distribution in a Poisson process with density $\sqrt{(1-\xi)_+}$. We will not give the technical details that are required to prove these results from the results above.

For tiling models with frozen and unfrozen regions, the tiling measure is a local Gibbs measure. That is, by rescaling in a region so that the lattice remains but the boundary conditions are forgotten, the measure governing the dimer configurations is a Gibbs measure. For domino tilings of the Aztec diamond, we show that we can recover the local Gibbs measure in the interior of the unfrozen region.

Theorem 2.8. *Choose the rescaling so that the white vertices are given by*

$$(x_1, x_2) = ([\alpha_1 n] + 2\xi_1 + 1, [\alpha_2 n] + 2\xi_2)$$

and the black vertices are given by

$$(y_1, y_2) = ([\alpha_1 n] + 2\eta_1, [\alpha_2 n] + 2\eta_2 + 1)$$

for $\alpha_1, \alpha_2 \in \text{int}(\mathcal{D})$ and for $\xi_1, \xi_2, \eta_1, \eta_2 \in \mathbb{Z}$. Then, the measure on domino tilings converges to weakly to $\mu_a(\log\sqrt{\alpha_1/(1-\alpha_1)}, \log\sqrt{\alpha_2/(1-\alpha_2)})$ where μ_a is defined in Section 2.5.

Our last result concerns the asymptotics of the fluctuations of the height function in the bulk. Following the well-established techniques for tiling models, we find that

Theorem 2.9. *For $0 < a < \infty$ fixed, the fluctuations of the height function in the interior $\mathcal{D}$ are given by the pullback of the Gaussian Free Field on $\mathbb{H}$.*

The proof uses the fact that the moments of the height function can be found using the knowledge of the inverse Kastelyn matrix as used in [6, 10, 25, 26, 27]. As a consequence, we have to compute the global asymptotics of the inverse Kasteleyn matrix. Tiling models with frozen and unfrozen regions, [3] gave an approach for proving the Gaussian free field for lozenge tilings models provided they are completely described by an interlaced particle system with densely packed initial configuration. Building on results from [34], [35] was able to prove universality of [3]. Much of the proof of Theorem 2.9 follows the approach taken in

[3] and so we omit some of the technical estimates as these can be found in [3, 35]. Other approaches for proving fluctuations of the height function arising from a tiling model have been considered in [12], where the author exploits a quadruple integral to bypass some rather technical estimates, and [11], where the author considers the characteristic function of the height function using the Cauchy Riemann operators. The proofs of the results of [26, 25] do not apply to domino tilings on the Aztec diamond due to the domino tilings studied there had the so-called *Temperley boundary conditions*.

2.8. **Overview of the Paper.** The rest of the paper is organized as follows. In Section 3, we prove that Theorem 2.3. In Section 4, we give the the proofs of Theorem 2.6, Theorem 2.7 and Theorem 2.8. The proof of Theorem 2.9 is given in Section 5. In Section 6, we give the relationship between the dimer correlation kernel and the particle correlation kernel, introduced in [19].

3. Discrete Setting

3.1. **Some Comments on Theorem 2.3.** Theorem 2.3 was first obtained in [16] for $a = 1$. The approach used was an explicit enumeration of $K^{-1}(w, b)2^{n(n+1)/2}$ which counts the number of signed perfect matchings with w and b removed from the Aztec diamond where the sign comes from adapting the Kasteleyn orientation for the removed vertices so that the number of counter clockwise edges per face is odd (alternatively, the product of the edge weights around each face is negative).

We can also give a version of the coupling function when the dimer model has weights r_1, r_2, r_3 and r_4 for the north, east, south and west dimers. However, the partition function of the dimer model is function of the ratio of the weights r_1/r_3 and r_2/r_4 which means the extra weights are superfluous.

3.2. **Proof of Theorem 2.3.**

Proof of Theorem 2.3. The matrix K^{-1} is uniquely determined by the specific choice of the Kasteleyn matrix, K. We only need to check that $KC = \mathbb{I}$ where $C_{x,y} = c(x, y)$. For $b, y \in \mathtt{B} \cap A_n$, we have

$$\begin{aligned} KC(b, y) &= \sum_{x \in \mathtt{W}} K(b, x)C(x, y) \\ &= \sum_{x \sim b} K(b, x)C(x, y) \end{aligned} \tag{3.1}$$

where $K(b, w)$ is given in (2.11). We have that the rows and columns of KC are indexed by black vertices. There are three cases to consider which are dependent on $b = (b_1, b_2)$; $0 < b_1 < 2n$, $b_1 = 0$ and $b_1 = 2n$. In each of the three cases, we set $j = (b_1 + b_2 - 1)/2$.

For $0 < b_1 < 2n$, we have that each entry of (3.1) is given by

$$(-1)^j \left(c(b + e_1, y) - c(b - e_1, y) - aic(b + e_2, y) + aic(b - e_2, y)\right). \tag{3.2}$$

For $y_1 \neq b_1$, we have that

$$(-1)^j \left(c(b + e_1, y) - c(b - e_1, y) - aic(b + e_2, y) + aic(b - e_2, y)\right) = 0 \tag{3.3}$$

which can be seen by directly manipulating the integrands of the functions $f_1(x,y)$ and $f_2(x,y)$, defined in (2.26) and (2.28). For $y_1 = b_1$, (3.2) is equal to

$$-\frac{(-1)^{\frac{b_1+3b_2+3y_1+y_2}{4}}}{2\pi i}\int_{\mathcal{E}_1} a^{\frac{y_2-b_2-2}{2}}(1+a^2)z^{\frac{y_2-b_2-2}{2}}\left(\frac{1}{a}+a+z\right)^{\frac{b_2-y_2-2}{2}}dz \tag{3.4}$$

$$=\begin{cases} -(-1)^{(y_1+y_2)} & b_2 = y_2 \\ 0 & \text{otherwise} \end{cases} \tag{3.5}$$

by using Lemma 3.1. As $(y_1+y_2) \mod 4$ is either 1 or 3, we have

$$KC(b,y) = \begin{cases} 1 & 0 < b_1 < 2n, y_1 = b_1 \\ 0 & 0 < b_1 < 2n, y_1 \neq b_2 \end{cases}. \tag{3.6}$$

For $b_1 = 0$, we have that each entry of (3.1) is given by

$$(-1)^j\left(c(b+e_1,y)) + aic(b-e_2,y)\right). \tag{3.7}$$

For $2 \leq y_1 \leq 2n$, (3.7) is equal to

$$\frac{(-1)^{\frac{3b_2+y_1+y_2}{4}}}{(2\pi i)^2}\int_{\mathcal{E}_2}\int_{\mathcal{E}_1}\frac{(1+a^2)}{w-z}\frac{w^{\frac{y_1}{2}}(a+z)^{\frac{b_2-1}{2}}(az-1)^{\frac{2n-1-b_2}{2}}}{(aw-1)^{\frac{2n+1-y_2}{2}}(a+w)^{\frac{y_2+1}{2}}}dz\,dw = 0 \tag{3.8}$$

because the function is analytic at $z = 0$.

For $b_1 = 0$ and $y_1 = 0$, (3.7) is equal to

$$\frac{(-1)^{\frac{3b_2+y_2}{4}}}{(2\pi i)^2}\int_{\mathcal{E}_2}\int_{\mathcal{E}_1}\frac{(1+a^2)}{w-z}\frac{(a+z)^{\frac{b_2-1}{2}}(az-1)^{\frac{2n-1-b_2}{2}}}{(aw-1)^{\frac{2n+1-y_2}{2}}(a+w)^{\frac{y_2+1}{2}}}dzdw \tag{3.9}$$

$$-\frac{(-1)^{\frac{3b_2+y_2}{4}}}{2\pi i}\int_{\mathcal{E}_1} a^{\frac{y_2-b_2-2}{2}}(1+a^2)z^{\frac{y_2-b_2-2}{2}}\left(\frac{1}{a}+a+z\right)^{\frac{b_2-y_2-2}{2}}dz \tag{3.10}$$

The first integral in equation (3.9) is zero because the function is analytic at $z = 0$. By Lemma 3.1, the second integral in (3.9) is equal to $-(-1)^{y_2} = 1$ when $b_2 = y_2$ and zero otherwise. Therefore, we have

$$KC(b,y) = \begin{cases} 1 & b_1 = 0, y_1 = b_1 \\ 0 & b_1 = 0, 2 \leq y_1 \leq 2n \end{cases} \tag{3.11}$$

For $b_1 = 2n$, we have that we have that each entry of (3.1) is given by

$$(-1)^j\left(c(b-e_1,y)) - aic(b+e_2,y)\right). \tag{3.12}$$

For $b_1 = 2n$ and $0 \leq y_1 \leq 2n-2$, (3.7) is equal to

$$-\frac{(-1)^{\frac{6n+3b_2+y_1+y_2}{4}}}{(2\pi i)^2}\int_{\mathcal{E}_2}\int_{\mathcal{E}_1}\frac{(1+a^2)}{w-z}\frac{w^{\frac{y_1}{2}}(a+z)^{\frac{b_2-1}{2}}(az-1)^{\frac{2n-1-b_2}{2}}}{z^n(aw-1)^{\frac{2n+1-y_2}{2}}(a+w)^{\frac{y_2+1}{2}}}dz\,dw \tag{3.13}$$

$$+\frac{(-1)^{\frac{6n+3b_2+y_1+y_2}{4}}}{2\pi i}\int_{\mathcal{E}_1} a^{\frac{y_2-b_2-2}{2}}(1+a^2)z^{\frac{y_2-b_2-2}{2}}\left(\frac{1}{a}+a+z\right)^{\frac{b_2-y_2-2}{2}}\left(\frac{1}{a}+z\right)^{-\frac{2n-y_1}{2}}dz \tag{3.14}$$

For the first integral in (3.13), we can compute the residue at $z = 0$ using the following integral:

$$-\frac{1}{2\pi i}\int_{\mathcal{E}_1}\frac{(a+z)^{\frac{x_2-1}{2}}(az-1)^{\frac{2n-1-x_2}{2}}}{z^n(w-z)}dz = -\frac{(a+w)^{\frac{x_2-1}{2}}(aw-1)^{\frac{2n-1-x_2}{2}}}{w^n}. \tag{3.15}$$

This follows from the fact that the sum of the exponents in the numerator is less than n and pushing the contour through infinity. Using (3.15) and the change of variables $w = z + 1/a$, the first integral in (3.13) becomes

$$-\frac{(-1)^{\frac{6n+3b_2+y_1+y_2}{4}}}{2\pi i}\int_{\mathcal{E}_1} a^{\frac{y_2-b_2-2}{2}}(1+a^2)z^{\frac{y_2-b_2-2}{2}}\left(\frac{1}{a}+a+z\right)^{\frac{b_2-y_2-2}{2}}\left(\frac{1}{a}+z\right)^{-\frac{2n-y_1}{2}}dz. \tag{3.16}$$

The above expression is exactly the negative of the second integral in (3.13).

For $b_1 = 2n$ and $y_1 = 2n$, (3.12) is equal to

$$-\frac{(-1)^{\frac{3b_2+y_2}{4}}}{(2\pi i)^2}\int_{\mathcal{E}_2}\int_{\mathcal{E}_1}\frac{(1+a^2)}{w-z}\frac{w^n(a+z)^{\frac{b_2-1}{2}}(az-1)^{\frac{2n-1-b_2}{2}}}{z^n(aw-1)^{\frac{2n+1-y_2}{2}}(a+w)^{\frac{y_2+1}{2}}}dz\,dw. \tag{3.17}$$

Using (3.15), we can compute the residue at $z = 0$ for (3.17) which gives

$$-\frac{(-1)^{\frac{3b_2+y_2}{4}}}{2\pi i}\int_{\mathcal{E}_2}(1+a^2)\frac{(a+w)^{\frac{b_2-y_2-2}{2}}}{(aw-1)^{\frac{y_2-b_2-2}{2}}}dw = \begin{cases} 1 & b_2 = y_2 \\ 0 & \text{otherwise} \end{cases} \tag{3.18}$$

using Lemma (3.1) with the change of variable $w = z + 1/a$. Therefore, we have

$$KC(b,y) = \begin{cases} 1 & b_1 = 2n, y_1 = b_1 \\ 0 & b_1 = 2n, 0 \le y_1 \le 2n-2 \end{cases}. \tag{3.19}$$

Combining (3.6), (3.11) and (3.19) shows that $K = C^{-1}$.

□

Lemma 3.1. *For $k \in \mathbb{Z}$,*

$$\frac{1}{2\pi i}\int_{|z|=1} z^{k-1}\left(\frac{1}{a}+a+z\right)^{-1-k}dz = \begin{cases} \frac{a}{1+a^2} & k = 0 \\ 0 & \textit{otherwise} \end{cases} \tag{3.20}$$

Proof. For $k = 0$, the left hand-side of (3.20) is equal to

$$\frac{1}{2\pi i}\int_{|z|=1}\frac{1}{z(\frac{1}{a}+a+z)}dz = \frac{a}{1+a^2}. \tag{3.21}$$

When $k > 0$, the integrand in (3.20) is analytic at $z = 0$ and so the left-hand-side of (3.20) is zero. When $k < 0$, we can move the contour to a small circle around $-(a + 1/a)$ and use the fact that the integrand is analytic inside. □

4. Asymptotics of Dimers

In this section, we will give the proofs of the results on the local asymptotics of the Aztec diamond. We start by proving Proposition 2.5 about thinned and thickened determinantal point processes.

Proof of Proposition 2.5. Let $\{y_j\}$ be the points of the determinantal point process with kernel K and let $\{n_j\}$ be independent Bernoulli random variables, $\mathbb{P}[n_j = 1] = \alpha$. Let $\mathbb{E}_K$ denote the expectation for the determinantal point process and $\mathbb{E}_n$ the expectation with respect to the Bernoulli random variables. Consider the thinned process. Then, by Fubini's theorem,

$$\mathbb{E}\left[e^{-\sum_j \psi(x_j)}\right] = \mathbb{E}_n\mathbb{E}_K\left[e^{-\sum_j n_j\psi(y_j)}\right] = \mathbb{E}_K\mathbb{E}_n\left[\prod_j(1-(1-e^{-n_j\psi(y_j)}))\right]$$

$$= \mathbb{E}_K\left[\prod_j(1-\mathbb{E}_n[1-e^{-n_j\psi(y_j)}])\right] = \mathbb{E}_K\left[\prod_j(1-\alpha\phi(y_j))\right] \tag{4.1}$$

$$= \det(I-\phi\alpha K 1_A). \tag{4.2}$$

which proves (2.31). Next, let $\{m_j\}$ be independent geometric random variables, $\mathbb{P}[m_j = k] = (1-\beta)\beta^{k-1}$, $k \geq 1$ and let $\mathbb{E}_m$ denote the expectation with respect to these random variables. Then

$$\mathbb{E}\left[e^{-\sum_j \psi(x_j)}\right] = \mathbb{E}_m\mathbb{E}_K\left[e^{-\sum_j m_j\psi(y_j)}\right] = \mathbb{E}_K\mathbb{E}_m\left[\prod_j(1-(1-e^{-n_j\psi(y_j)}))\right]$$

$$= \mathbb{E}_K\left[\prod_j(1-\frac{\phi(y_j)}{1-\beta-\beta\phi(y_j)})\right] = \det\left(I-\frac{\phi}{1-\beta-\beta\phi}K1_A\right), \tag{4.3}$$

since

$$\mathbb{E}\left[1-e^{-m_j\psi(y_j)}\right] = 1-(1-\beta)\sum_{k=0}^{\infty}\beta^{k-1}e^{-k\psi(y_j)}$$

$$= \frac{1-e^{-\psi(y_j)}}{1-\beta e^{-\psi(y_j)}} = \frac{\phi(y_j)}{1-\beta-\beta\phi(y_j)}. \tag{4.4}$$

This proves (2.32). □

Proof of Theorem 2.6. By Lemma 2.4 the south domino process on the line $y = r$ is a determinantal point process with kernel L given by (2.29). Let us first consider this process in a neighbourhood of the northern boundary, when $r = [(1-k^2u(k))n]$, $k > 0$. (Below we will often neglect the integer part in this and in other expressions. It is not difficult to see that this is unimportant.) The kernel can be written

$$L(x_1,x_2) = -\frac{1}{(2\pi i)^2}\int_{\Gamma_1}dz\int_{\Gamma_2}dw\frac{w^{x_2-nu(k)}}{z^{x_1-nu(k)}}\frac{1}{(a+w)(w-z)}e^{ng(z)-ng(w)}, \tag{4.5}$$

where

$$g(z) = (1-k^2u(k))\log(a+z) + k^2u(k)\log(az-1) - u(k)\log z. \tag{4.6}$$

Here we choose the argument in the logarithms in the interval $(0, 2\pi)$. We see that when $u(k)$ is given by (2.19), $g(z)$ has a double zero at

$$z_c = \frac{1}{a+k\sqrt{1+a^2}}. \tag{4.7}$$

We can now use a saddle-point argument to analyze the relevant asymptotics of (4.5) and since this is a fairly standard Airy kernel asymptotics saddle point analysis we will not go into the details. For the integration contours in (4.5) we have chosen the steepest descent contours given by the level lines of the imaginary part of $g(z)$ starting at z_c. It can be seen that we will have two ascending contours for the real part of $g(z)$ which will leave in the directions $e^{\pm\pi i/3}$ and go to infinity. We will choose these for our w-integration. We will have two descending contours going from z_c to $-a$ leaving in the directions $e^{\pm 2\pi i/3}$ and we use these for the z-integration. If we have the scaling

$$x_1 = [nu(k) - \lambda n^{1/3}\xi], \quad x_2 = [nu(k) - \lambda n^{1/3}\eta], \tag{4.8}$$

then

$$\lim_{n\to\infty} -\lambda n^{1/3} z_c^{x_1-x_2} L(x_1.x_2) = \alpha \frac{1}{(2\pi i)^2}\int_\Gamma dz \int_\Gamma dw \frac{1}{i(z+w)} e^{iz^3/3 + i\xi z + iw^3/3 + i\eta w} \tag{4.9}$$

$$= \alpha K_{\mathrm{Ai}}(\xi,\eta) \tag{4.10}$$

uniformly for ξ, η in a compact subset of $\mathbb{R}$, where $\alpha = z_c/(z_c + a)$. Here Γ is given by $z(t) = -te^{(\pi-\theta)i}$, $t < 0$ and $z(t) = te^{i\theta}$, $t \geq 0$, with a fixed $0 < \theta < \pi/3$. Furthermore, λ is given by

$$\lambda = z_c(-g^{(3)}(z_c)/2)^{1/3}. \tag{4.11}$$

A computation gives (2.36). To prove the result in Theorem 2.6 we observe that, with $\phi = 1 - e^{-\psi}$ and $[n] = \{1, \dots, n\}$,

$$\mathbb{E}\left[e^{-\sum_j \psi(\xi_j)}\right] = \mathbb{E}\left[\prod_j \left(1 - \phi\left(\frac{nu(k) - x_j}{\lambda n^{1/3}}\right)\right)\right] \tag{4.12}$$

$$= \sum_{m=0}^{n} \frac{(-1)^m}{m!} \sum_{x_1,\dots,x_m \in [n]} \prod_{j=1}^{m} \phi\left(\frac{nu(k) - x_j}{\lambda n^{1/3}}\right) \det(L(x_i, x_j))_{m\times m}. \tag{4.13}$$

Using the uniform convergence in (4.9) and Hadamard's inequality we see that (4.12) converges to

$$\sum_{m=0}^{n} \frac{(-1)^m}{m!} \int_{\mathbb{R}^m} \prod_{j=1}^{m} \phi(\xi_j) \det\left(\alpha K_{\mathrm{Ai}}(\xi_i, \xi_j)\right)_{m\times m} d^m\xi = \det\left(I - \phi\alpha K_{\mathrm{Ai}} 1_A\right), \tag{4.14}$$

for every $\psi \in C_c^+(\mathbb{R})$, where $A = \operatorname{supp}\phi = \operatorname{supp}\psi$. This proves the weak convergence claimed in the theorem.

We turn now to the south domino process close to the southern boundary. Take r as before but with $k \in (-a^{-1}(1+a^2)^{1/2}, -a(1+a^2)^{-1/2})$. We can write

$$L(x_1, x_2) = \frac{1}{(2\pi i)^2}\int_{\gamma_{r_1}} dz \int_{\gamma_{r_2}} dw \frac{w^{x_2}}{z^{x_1}} \frac{(a+z)^r (az-1)^{n-r}}{(a+w)^{r+1}(aw-1)^{n-r}} \frac{1}{w-z}, \tag{4.15}$$

where γ_r is $|z| = r$ positively oriented and $0 < r_1 < r_2$, $a < r_2 < 1/a$. Let $a < r_3 < r_1$, $r_3 < 1/a$ and set

$$\tilde{L}(x_1, x_2) = \frac{z_c^{x_1-x_2}}{(2\pi i)^2}\int_{\gamma_{r_1}} dz \int_{\gamma_{r_3}} dw \frac{w^{x_2}}{z^{x_1}} \frac{(a+z)^r (az-1)^{n-r}}{(a+w)^{r+1}(aw-1)^{n-r}} \frac{1}{w-z}. \tag{4.16}$$

Here z_c is again given by (4.7). Note that now we have $z_c \in (-\infty, -a)$. If we move the w-contour through the z-contour we obtain

$$z_c^{x_1-x_2} L(x_1, x_2) = \frac{z_c^{x_1-x_2}}{(2\pi i)} \int_{\gamma_{r_1}} \frac{z^{x_2-x_1}}{z+a}\, dz + \tilde{L}(x_1, x_2). \tag{4.17}$$

The parameter β is given by $\beta = -a/z_c$ and we see that $0 < \beta < 1$. Set

$$M(x_1, x_2) = -\beta^{x_2-x_1} \mathbb{1}_{(x_1<x_2)}, \tag{4.18}$$

where $\mathbb{1}_{(x_1<x_2)}$ is equal to one if $x_1 < x_2$ and is equal to zero otherwise. Then (4.17) gives

$$z_c^{x_1-x_2} L(x_1, x_2) = \delta_{x_1 x_2} - M(x_1, x_2) + \tilde{L}(x_1, x_2). \tag{4.19}$$

A correlation kernel L^* for the dual point process is given by

$$L^*(x_1, x_2) = \delta_{x_1 x_2} - z_c^{x_1-x_2} L(x_1, x_2) = M(x_1, x_2) - \tilde{L}(x_1, x_2). \tag{4.20}$$

If $x_1, x_2, \ldots$ are the points in the dual point process we want to look at

$$\mathbb{E}\left[\prod_j \exp\left(-\sum_j \psi\left(\frac{x_j - nu(k)}{\lambda n^{1/3}}\right)\right)\right] = \det(I - fL^* g) \tag{4.21}$$

where the Fredholm determinant is on $\ell^2(\{1, \ldots, n\})$ and so is actually a determinant of a finite matrix. Here we have introduced $f(x) = \phi((\lambda n^{1/3})^{-1}(x - nu(k)))$ and $g(x) = 1_A((\lambda n^{1/3})^{-1}(x - nu(k)))$. Now, by (4.20), we have

$$\det(I - fL^* g) = \det(I - fL^*) = \det(I - fM + f\tilde{L}) \tag{4.22}$$

$$= \det(I - fM) \det(I + (I - fM)^{-1} f\tilde{L}) = \det(I + \sum_{j=0}^{n} (fM)^j f\tilde{L}) \tag{4.23}$$

$$= \det\left(I + f \sum_{j=0}^{n} (Mf)^j \tilde{L} g\right), \tag{4.24}$$

since M is idempotent, $M^{n+1} = 0$. Set

$$R = \sum_{j=1}^{n} (Mf)^j \tilde{L}. \tag{4.25}$$

Then, by (4.22), we have

$$\det(I - fL^* g) = \det(I - f(R + \tilde{L})g). \tag{4.26}$$

In order to prove the result in Theorem 2.6 it suffices to show that, with the scaling (4.8),

$$\lambda n^{1/3}(R + \tilde{L})(x_1, x_2) \to -\frac{1}{1 - \mu + \mu\phi(\xi)} K_{\mathrm{Ai}}(\xi, \eta) \tag{4.27}$$

uniformly for ξ, η in a compact subset of $\mathbb{R}$ as $n \to \infty$. We will prove this under the assumption that ψ is also continuously differentiable, which suffices to show the weak convergence of the point process.

We will make use of the following fact which again is proved by a saddle point argument very similar to the one discussed above. The only difference is in the choice of contours. As integration contours we will again choose level lines of the imaginary part of $g(z)$ starting at z_c. It can be seen that we will have two ascending contours for the real part of $g(z)$ which

will leave in the directions $e^{\pm\pi i/3}$ and go to 0. We will choose these for our w-integration. We will have two descending contours going from z_c to $1/a$ leaving in the directions $e^{\pm 2\pi i/3}$ and we use these for the z-integration.

Let x_1, x_2 be as in (4.8), $r = [(1-k^2u(k))n]$, $k \in (-a(1+a^2)^{-1/2}, -a^{-1}(1+a^2)^{1/2})$ and $a < r_3 < 1/a$, $r_3 < r_1$. Then, we have

(4.28)
$$\frac{\lambda n^{1/3} z_c^{x_1-x_2}}{(2\pi i)^2} \int_{\gamma_{r_1}} dz \int_{\gamma_{r_3}} dw\, F(z) \frac{w^{x_2}}{z^{x_1}} \frac{(a+z)^r (az-1)^{n-r}}{(a+w)^{r+1}(aw-1)^{n-r}} \frac{1}{w-z} \to -\frac{D}{1-\beta} K_{\mathrm{Ai}}(\xi,\eta)$$

uniformly for ξ, η in compacts as $n \to \infty$, for $F(z) = 1$ or $F(z) = \beta z_c/(z - \beta(1-f(x_1))z_c)$, where $D = F(z_c)$.

By expanding M and rearranging the sum, we have

$$\begin{aligned} R(x_1,x_2) &= \sum_{j=1}^{n} (Mf)^j \tilde{L}(x_1,x_2) \\ &= \sum_{j=1}^{n} (-1)^j \sum_{y_1,\dots,y_j \in [n]} \beta^{y_j - x_1} \mathbb{1}_{(x_1<y_1)} \dots \mathbb{1}_{(y_{j-1}<y_j)} f(y_1)\dots f(y_j) \tilde{L}(y_j,x_2) \\ &= \sum_{j=1}^{n} (-1)^j \sum_{t=j}^{n-x_1} \beta^t f(x_1+t) \tilde{L}(x_1+t,x_2) \sum_{x_1<y_1<\dots<y_{j-1},x_1+t} f(y_1)\dots f(y_{j-1}). \end{aligned}$$

Let $e_j(x_1,\dots,x_{t-1})$ be the j:th elementary symmetric polynomial in $t-1$ variables and write $f = (f(x_1+1),\dots,f(x_1+t-1))$. By interchanging the sums, we obtain

$$\begin{aligned} R(x_1,x_2) &= -\sum_{t=1}^{n-x_1} \beta^t f(x_1+t) \tilde{L}(x_1+t,x_2) \sum_{j=0}^{t-1} (-1)^{j-1} e_{j-1}(f) \\ &= -\sum_{t=1}^{n-x_1} \beta^t f(x_1+t) \tilde{L}(x_1+t,x_2) \prod_{j=1}^{t-1} (1-f(x_1+j)). \end{aligned} \tag{4.29}$$

Set

$$T(x_1,x_2) = -\sum_{t=1}^{n-x_1} \beta^t f(x_1)(1-f(x_1)^{t-1} \tilde{L}(x_1+t,x_2). \tag{4.30}$$

We then have the following

Claim 1. *For all ξ, η in a compact subset of $\mathbb{R}$ there is a constant C such that if we have the scaling (4.8) then*

$$|\lambda n^{1/3}(R-T)(x_1,x_2)| \le \frac{C}{n^{1/3}}. \tag{4.31}$$

We will prove the claim below. Using (4.16) we see that

(4.32)

$$\begin{aligned}
T(x_1,x_2) &= -\sum_{t=1}^{n-x_1}\beta^t f(x_1)(1-f(x_1))^{t-1}\frac{z_c^{x_1-x_2}}{(2\pi i)^2}\int_{\gamma_{r_1}}dz\int_{\gamma_{r_3}}dw\left(\frac{z_c}{z}\right)^t\\
&\times\frac{w^{x_2}}{z^{x_1}}\frac{(a+z)^r(az-1)^{n-r}}{(a+w)^{r+1}(aw-1)^{n-r}}\frac{1}{w-z}\\
&= -\frac{f(x_1)}{1-f(x_1)}\frac{z_c^{x_1-x_2}}{(2\pi i)^2}\int_{\gamma_{r_1}}dz\int_{\gamma_{r_3}}dw\frac{\beta(1-f(x_1))z_c/z-(\beta(1-f(x_1))z_c/z)^{n-x_1+1}}{1-\beta(1-f(x_1))z_c/z}\\
&\times\frac{w^{x_2}}{z^{x_1}}\frac{(a+z)^r(az-1)^{n-r}}{(a+w)^{r+1}(aw-1)^{n-r}}\frac{1}{w-z}\\
&= -f(x_1)\frac{z_c^{x_1-x_2}}{(2\pi i)^2}\int_{\gamma_{r_1}}dz\int_{\gamma_{r_3}}dw\frac{\beta z_c}{z-\beta(1-f(x_1))z_c}\frac{w^{x_2}}{z^{x_1}}\frac{(a+z)^r(az-1)^{n-r}}{(a+w)^{r+1}(aw-1)^{n-r}}\frac{1}{w-z}.
\end{aligned}$$

It now follows from (4.28) that

$$\lambda n^{1/3}T(x_1,x_2)\to\frac{\beta\phi(\xi)}{1-\beta(1-\phi(\xi))}\frac{1}{1-\beta}K_{\mathrm{Ai}}(\xi,\eta) \tag{4.33}$$

uniformly as $n\to\infty$. If we combine this with (4.31) and the fact that, again by (4.28) with $F(z)=1$, that

$$\lambda n^{1/3}\tilde{L}(x_1,x_2)\to-\frac{1}{1-\beta}K_{\mathrm{Ai}}(\xi,\eta) \tag{4.34}$$

we obtain (4.27), which is what we wanted to prove.

It remains to prove the claim. We will use the following two facts. If ξ,η belongs to a compact subset, there is a constant $B>0$ and a constant C such that if we have the scaling (4.8) then: (i) $f(x_1+j)=0$ if $j\notin[-Bn^{1/3},Bn^{1/3}]$ and (ii) $|\lambda n^{1/3}\tilde{L}(x_1+t,x_2)|\le C$ for all $t\in[-Bn^{1/3},Bn^{1/3}]$. That (i) holds follows immediately from the fact that ϕ has compact support, and (ii) follows from (4.28) in the case $F(z)=1$ since we have uniform convergence.

Now, since ϕ is continuously differentiable and has compact support,

$$\begin{aligned}
&\left|\prod_{j=1}^{t-1}(1-f(x_1+t))-\prod_{j=1}^{t-1}(1-f(x_1))\right|\\
&\le\left|\sum_{\ell=1}^{t-1}(1-f(x_1)^{\ell-1}(f(x_1+\ell)-f(x_1))\prod_{j=\ell+1}^{t-1}(1-f(x_1+j))\right|\\
&\le\sum_{\ell=1}^{t-1}|f(x_1+\ell)-f(x_1))|\\
&=\sum_{\ell=1}^{t-1}\left|\phi\left(\frac{[nu(k)+\lambda n^{1/3}]+\ell-nu(k)}{\lambda n^{1/3}}\right)-\phi\left(\frac{[nu(k)+\lambda n^{1/3}]-nu(k)}{\lambda n^{1/3}}\right)\right|\\
&\le\sum_{\ell=1}^{t-1}\frac{C\ell}{n^{1/3}}\le\frac{Ct^2}{n^{1/3}},
\end{aligned} \tag{4.35}$$

for some constant C. Thus,

$$\begin{aligned} &|\lambda n^{1/3}(R-T)(x_1,x_2)| \\ &\leq \sum_{t=1}^{n-x_1} \beta^t |f(x_1+t)||\lambda n^{1/3}\tilde{L}(x_1+t,x_2)| \left| \prod_{j=1}^{t-1}(1-f(x_1+t)) - \prod_{j=1}^{t-1}(1-f(x_1)) \right| \\ &\leq \frac{C}{n^{1/3}} \sum_{t=1}^{n-x_1} \beta^t t^2 \leq \frac{C}{n^{1/3}}, \end{aligned} \tag{4.36}$$

since $0 < \beta < 1$.

□

Above we have been concerned with the behavior of the south dominos at the boundary of the frozen region. We can also consider the behavior of the south dominos as we enter the bulk but still stay close to the boundary at a macroscopic scale. We then get as a scaling limit the thinned sine kernel point process with the same parameter α. We will not go into the details.

Next we will give the proof of Theorem 2.7 which is concerned with the case when a grows with n but not too fast. In the case when a instead goes to zero with n but not to fast we will have convergence to the Airy kernel point process at the northern boundary for the south domino process. Note that the thinning parameter $\alpha \to 1$ as $a \to 0$. If $a = \gamma/n$ for some fixed $\gamma > 0$ then we get instead the discrete Bessel kernel in the limit as $n \to \infty$. Again we will not go into the details.

Proof of Theorem 2.7. Set

$$L^*(x_1,x_2) = z_c^{x_1-x_2} L(x_1,x_2), \tag{4.37}$$

with L as in (4.5) and z_c given by (4.7). Take $\phi \in C_c(\mathbb{R})$, $0 \leq \phi \leq 1$ and let

$$f(x) = \phi\left(\frac{nu(k) + c(a)n^{1/3} - x}{c(a)n^{1/3}} \right) \tag{4.38}$$

for $x \in [n] = \{1, \dots, n\}$. Furthermore, define

$$M_n(\xi,\eta) = -c(a)n^{1/3} L_n^*([nu(k) - c(a)n^{1/3}(\xi-1)], [nu(k) - c(a)n^{1/3}(\eta-1)]). \tag{4.39}$$

Set

$$I_j = \left(\frac{nu(k) + c(a)n^{1/3} - (j+1)}{c(a)n^{1/3}}, \frac{nu(k) + c(a)n^{1/3} - j}{c(a)n^{1/3}} \right], \tag{4.40}$$

for $j \in \mathbb{Z}$, and

$$\tilde{\phi}_n(\xi) = \phi\left(\frac{nu(k) + c(a)n^{1/3} - j)}{c(a)n^{1/3}} \right) \tag{4.41}$$

for $\xi \in I_j$, $j \in \mathbb{Z}$. LetA be a compact subset of the real line such that $\operatorname{supp} \tilde{\phi}_n \subseteq A$ for all n. Then,

$$\mathbb{E}\left[\prod_j (1-\phi(\xi_j))\right] = \sum_{m=0}^{n} \frac{(-1)^m}{m!} \sum_{x_1,\dots,x_m \in [n]} \prod_{j=1}^{m} f(x_j) \det(L^*(x_i,x_j))_{m\times m} \tag{4.42}$$

$$= \sum_{m=0}^{n} \frac{(-1)^m}{m!} \int_{\mathbb{R}^m} \prod_{j=1}^{m} \tilde{\phi}_n(\xi_j) \det(M_n(\xi_i,\xi_j))_{m\times m}\, d^m\xi \tag{4.43}$$

$$= \det(I - \tilde{\phi}_n M_n 1_A)_{L^2(\mathbb{R})}. \tag{4.44}$$

Assume that we can show that

$$||\tilde{\phi}_n M_n 1_A||_2 \to 0 \tag{4.45}$$

as $n \to \infty$, where $||\cdot||_2$ is the Hilbert-Schmidt norm, and

$$M_n(\xi,\xi) \to \sqrt{(1-\xi)_+} \tag{4.46}$$

uniformly for $\xi \in A$ as $n \to \infty$. The result then follows from (4.42) in the following way. if the operators B_n on $L^2(\mathbb{R})$ are trace class then the $\det_2(I+B_n)$ determinant and the Fredholm determinant $\det(I+B_n)$ are related by

$$\det(I+B_n) = e^{\operatorname{tr} B_n} \det_2(I+B_n). \tag{4.47}$$

Also, if we have $||B_n||_2 \to 0$ as $n \to \infty$, then we have $\det_2(I+B_n) \to 1$ as $n \to \infty$, see [15]. Hence

$$\det(I - \tilde{\phi}_n M_n 1_A) = e^{\operatorname{tr} \tilde{\phi}_n M_n 1_A} \det_2(I - \tilde{\phi}_n M_n 1_A). \tag{4.48}$$

It follows from (4.45) that $\det_2(I - \tilde{\phi}_n M_n 1_A) \to 0$ as $n \to \infty$, and from (4.46) that

$$\operatorname{tr} \tilde{\phi}_n M_n 1_A = \int_{\mathbb{R}} \tilde{\phi}_n(\xi) M_n(\xi,\xi)\, d\xi \to \int_{\mathbb{R}} \phi(\xi)\sqrt{(1-\xi)_+}\, d\xi, \tag{4.49}$$

as $n \to \infty$. Thus, by (4.42) and (4.48),

$$\lim_{n\to\infty} \mathbb{E}\left[\prod_j (1-\phi(\xi_j))\right] = e^{-\int_{\mathbb{R}} \phi(\xi)\sqrt{(1-\xi)_+}\, d\xi}, \tag{4.50}$$

which is what we wanted to prove.

We turn now to the asymptotic analysis of M_n and the proof of (4.45) and (4.46). We will denote by C a generic constant that can depend on k and d in Claim 2 but not on n or a. Let λ be given by (2.36) and define

$$M_n^{(1)}(\xi,\eta) = -\lambda n^{1/3} L^*([nu(k) - \lambda n^{1/3}\xi], [nu(k) - \lambda n^{1/3}\eta]) \tag{4.51}$$

Claim 2. *Let α be given by (2.35) and fix $d > 0$. Then*

$$|M_N^{(1)}(\xi,\eta) - \alpha K_{Ai}(\xi,\eta)| \le \frac{C}{a^2} \tag{4.52}$$

for all $\xi, \eta \in [-da^{4/3}, da^{4/3}]$.

We will prove the claim below. Set $\tilde{c}(a) = c(a)/\lambda$ and note that $\tilde{c}(a) \sim \pi^{2/3} a^{4/3}(1+k)^{2/3}$ as $a \to \infty$. Then, we find that

$$M_n(\xi+1,\eta+1) = \tilde{c}(a) M_N^{(1)}(\tilde{c}(a)\xi, \tilde{c}(a)\eta). \tag{4.53}$$

Thus, with an appropriate fixed $d_1 > 0$, we have

(4.54)
$$\begin{aligned}||\tilde{\phi}_n M_n 1_A||_2 &= \int_{\mathbb{R}^2} \tilde{\phi}_n(x)^2 M_n(x,y)^2 1_A(y)\,dxdy \le \int_{[-d_1,d_1]^2} M_n(\xi+1,\eta+1)^2\,d\xi d\eta \\ &= \tilde{c}(a)^2 \int_{[-d_1,d_1]^2} M_N^{(1)}(\tilde{c}(a)\xi,\tilde{c}(a)\eta)^2\,d\xi d\eta = \int_{[-da^{4/3},da^{4/3}]^2} M_N^{(1)}(\xi,\eta)^2\,d\xi d\eta,\end{aligned}$$

where $d = d_1\pi^{2/3}(1+k)^{2/3}$. Using (4.52) we see that

$$||\tilde{\phi}_n M_n 1_A||_2 \le 2\alpha^2 \int_{[-da^{4/3},da^{4/3}]^2} K_{\mathrm{Ai}}(\xi,\eta)^2\,d\xi d\eta + 2d^2(a^{4/3}a^{-2})^2. \tag{4.55}$$

Now $a^{-4/3} \to 0$, since $a = a(n) \to \infty$ as $n \to \infty$, and we see that in order to prove (4.45) it remains to control the integral in (4.55). If we use the identity

$$\int_{-\infty}^{\infty} K_{\mathrm{Ai}}(x,y)^2\,dy = K_{\mathrm{Ai}}(x,x), \tag{4.56}$$

and

$$K_{\mathrm{Ai}}(x,x) = \mathrm{Ai}\,'(x)^2 - x\mathrm{Ai}(x)^2 \tag{4.57}$$

we see that

$$\begin{aligned}&2\alpha^2 \int_{[-da^{4/3},da^{4/3}]^2} K_{\mathrm{Ai}}(\xi,\eta)^2\,d\xi d\eta \le 2\alpha^2 \int_{-da^{4/3}}^{da^{4/3}} K_{\mathrm{Ai}}(\xi,\xi)\,d\xi \\ &\le 2\alpha^2 \int_{-da^{4/3}}^{\infty} \mathrm{Ai}\,'(\xi)^2 - x\mathrm{Ai}(\xi)^2\,d\xi \qquad (4.58) \\ &= \frac{2\alpha^2}{3}\left[2(da^{4/3})^2\mathrm{Ai}^{\,2}(-da^{4/3}) + 2da^{4/3}\mathrm{Ai}\,'(-da^{4/3})^2 - \mathrm{Ai}(-da^{4/3})\mathrm{Ai}\,'(-da^{4/3})\right].\end{aligned}$$

Now, as $r \to \infty$ we have

(4.59)
$$\mathrm{Ai}(-r) = \frac{1}{\sqrt{\pi}} r^{-1/4}\sin\left(\frac{2}{3}r^{3/2} + \frac{\pi}{4}\right) + \ldots, \quad \mathrm{Ai}\,'(-r) = \frac{1}{\sqrt{\pi}} r^{1/4}\cos\left(\frac{2}{3}r^{3/2} + \frac{\pi}{4}\right) + \ldots$$

and hence, since $\alpha \sim (1+k)^{-1}a^{-2}$ for large a, we obtain the bound

$$2\alpha^2 \int_{[-da^{4/3},da^{4/3}]^2} K_{\mathrm{Ai}}(\xi,\eta)^2\,d\xi d\eta \le Ca^{-4}(da^{4/3})^{3/2} \le Ca^{-2} \tag{4.60}$$

and since $a = a(n) \to \infty$ we have proved (4.45).

It follows from (4.52) and (4.53) that

$$|M_n(\xi,\xi) - \alpha\tilde{c}(a)K_{\mathrm{Ai}}(\tilde{c}(a)(\xi-1),\tilde{c}(a)(\xi-1))| \le Ca^{4/3}a^{-2} = Ca^{-2/3} \tag{4.61}$$

for all ξ in a compact interval, and since $a \to \infty$ as $n \to \infty$, (4.46) follows by using (4.57) and standard asymptotic formulas for the Airy function and its derivative.

It remains to prove Claim 2. Let $\gamma > 0$ be given by $\gamma^3 g^{(3)}(z_c) = -2$ and recall that $\lambda = z_c/\gamma$. Let $g(z)$ be defined by (4.6) and write

$$f_\xi(\zeta) = \lambda n^{1/3}\xi\log\left(1 + \frac{\gamma\zeta}{z_c n^{1/3}}\right) \tag{4.62}$$

and

$$F_\xi(\zeta) = f_\xi(\zeta) + n(g(z_c + \gamma\zeta n^{-1/3}) - g(z_c)). \tag{4.63}$$

If we use (4.5) and make the change of variables $z = z_c + \gamma\zeta n^{-1/3}$, $w = z_c + \gamma\omega n^{-1/3}$ we obtain

$$M_n^{(1)}(\xi,\eta) = \frac{\alpha}{(2\pi i)^2}\int_{\mathcal{C}} d\zeta \int_{\mathcal{D}} d\omega \frac{a + z_c}{(a + z_c + \gamma\omega n^{-1/3})(\omega - \zeta)} e^{F_\xi(\zeta) - F_\eta(\omega)}, \tag{4.64}$$

where $\mathcal{C}$ and $\mathcal{D}$ are the images of the steepest descent contours in theorem 2.6. If $|\omega| \geq a^2 n^{1/3}$ we have the estimate

$$\left| e^{-F_\eta(\omega)} \right| \leq C^n a^{2n} \left| \frac{n^{1/3}}{a^{2/3}\omega} \right|^{n/2} \tag{4.65}$$

for all sufficiently large n. $\mathcal{C}$ will lie inside $|\zeta| \leq a^2 n^{1/3}$, and using (4.65) and the estimates we describe below for the ζ-integration, we see that we can replace $\mathcal{D}$ by the part of $\mathcal{D}$ that lies inside $|\omega| \leq a^2 n^{1/3}$. We denote this part by $\mathcal{D}$ also for simplicity.

Let $\mathcal{C}_1^*$ be the part of $\mathcal{C}$ in the disk $|\zeta| \leq n^{1/15}$, $\mathcal{C}_2^*$ the part in the annulus $n^{1/15} \leq |\zeta| \leq n^{7/45}$ and $\mathcal{C}_3^*$ the part in $|\zeta| \geq n^{7/45}$. Let $\mathcal{C}_i$ and $\bar{\mathcal{C}}_i$ be the parts of $\mathcal{C}_i^*$ that lie in the upper and lower half plane respectively. We make the analogous definitions for $\mathcal{D}$. We will consider estimates of $F_\xi(\zeta)$ on $\mathcal{C}_i$, $i = 1, 2, 3$. The estimates on $\bar{\mathcal{C}}_i$ are the same by symmetry and the estimates on $\mathcal{D}$ are analogous. The estimates that we need are

$$\operatorname{Re} n(g(z_c + \gamma\zeta n^{-1/3}) - g(z_c)) \leq -\frac{1}{6}|\zeta|^3 \tag{4.66}$$

for all $\zeta \in \mathcal{C}_1 + \mathcal{C}_2$ and

$$\operatorname{Re} n(g(z_c + \gamma\zeta n^{-1/3}) - g(z_c)) \leq -\frac{1}{6} n^{7/15} \tag{4.67}$$

for all $\zeta \in \mathcal{C}_3$ and n sufficiently large. To see this note that we can write

$$n(g(z_c + \gamma\zeta n^{-1/3}) - g(z_c)) = -\frac{1}{3}\zeta^3 + h_1(\zeta), \tag{4.68}$$

where

$$h_1(\zeta) = \frac{\gamma^4}{6n^{1/3}} \int_0^\zeta g^{(4)}(z_c + \frac{\gamma s}{n^{1/3}})(\zeta - s)^3\, ds. \tag{4.69}$$

Now, if we have $|\zeta| \leq n^{7/45}$, then

$$|h_1(\zeta)| \leq C a^{2/3} n^{-1/3} |\zeta|^4. \tag{4.70}$$

The estimate (4.70) follows from the fact that

$$|g^{(4)}(z_c + \frac{\gamma s}{n^{1/3}})| \leq C a^2 \tag{4.71}$$

for $|s| \leq n^{7/45}$ since $\gamma \leq C a^{-1/3}$. If we have $\zeta \in \mathcal{C}_1 + \mathcal{C}_2$, then $0 = -\frac{1}{3}\operatorname{Im}\zeta^3 + \operatorname{Im} h_1(\zeta)$ and if we write $\zeta = re^{i\theta}$ this gives $r^3 \sin 3\theta = 3\operatorname{Im} h_1(re^{i\theta})$ and hence, by (4.70),

$$|\sin 3\theta| \leq C a^{2/3} n^{-1/3} r \leq C n^{-1/9}. \tag{4.72}$$

Since $\mathcal{C}_1$ leaves z_c in the direction $e^{2\pi i/3}$ we must have $\cos 3\theta \geq 2/3$ for all large n. Thus

$$\mathrm{Re} n(g(z_c+\gamma\zeta n^{-1/3})-g(z_c)) = -\frac{1}{3}|\zeta|^3\cos 3\theta + \mathrm{Re}h_1(\zeta) \tag{4.73}$$

$$\leq -\frac{2}{9}|\zeta|^3(1-Ca^{2/3}n^{-1/3}|\zeta|) \leq -\frac{1}{6}|\zeta|^3 \tag{4.74}$$

if $\zeta \in \mathcal{C}_1+\mathcal{C}_2$ and n is large. This proves (4.66). Since $\mathrm{Re}\, n(g(z_c+\gamma\zeta n^{-1/3})-g(z_c))$ is decreasing as we move along $\mathcal{C}$ in the upper half plane starting at z_c we see that the value on $\mathcal{C}_3$ must be $\leq -n^{7/15}/6$ by using the estimate (4.66) at the point where $\mathcal{C}$ meets $|\zeta| = n^{7/15}$ (the endpoint of $\mathcal{C}_2$). This proves (4.67).

We can write

$$f_\xi(\zeta) = \xi\zeta + \xi h_2(\zeta), \tag{4.75}$$

where

$$h_2(\zeta) = -\frac{1}{\lambda n^{1/3}}\int_0^\zeta \frac{\zeta - s}{(1+s/\lambda n^{1/3})^2}\,ds, \tag{4.76}$$

and we see that if $|\zeta| \leq n^{7/45}$, then

$$|h_2(\zeta)| \leq Ca^{2/3}n^{-1/3}|\zeta|^2. \tag{4.77}$$

We start by estimating $F_\xi(\zeta)$ on $\mathcal{C}_3$. If $\zeta \in \mathcal{C}_3$ then $|\zeta| \leq a^2 n^{1/3}$ and hence

$$\mathrm{Re} f_\xi(\zeta) = \lambda\xi n^{1/3}\log\left|1+\frac{\zeta}{\lambda n^{1/3}}\right| \leq Cn^{6/15}\log n \tag{4.78}$$

and combining this with (4.67) we see that $\mathrm{Re}F_\xi(\zeta) \leq -\frac{1}{12}n^{7/15}$ for large n and hence the contribution from $\mathcal{C}_3$ is negligible.

Since $|\xi| \leq Ca^{4/3}$ and $a \leq Cn^{1/10}$ we see that if $\zeta \in \mathcal{C}_2$, then $\mathrm{Re}f_\xi(\zeta) \leq Cn^{1/10}|\zeta|$. Combining this with (4.66) we see that $\mathrm{Re}F_\xi(\zeta) \leq -|\zeta|^3/12$ for n large and hence the contribution from $\mathcal{C}_2$ is negligible.

Thus, with an error that is much smaller than Ca^{-2}, we can replace $M_n^{(1)}(\xi,\eta)$ by

$$\tilde{M}_n^{(1)}(\xi,\eta) = \frac{\alpha}{(2\pi i)^2}\int_{\mathcal{C}_1+\bar{\mathcal{C}_1}} d\zeta \int_{\mathcal{D}_1+\bar{\mathcal{D}}_1} d\omega \frac{a+z_c}{(a+z_c+\gamma\omega n^{-1/3})(\omega-\zeta)} e^{F_\xi(\zeta)-F_\eta(\omega)} \tag{4.79}$$

Set $\delta_n = a(n)/n^{1/10}$. By assumption $\delta_n \to 0$ as $n\to\infty$. If $|\zeta| \leq n^{1/15}$ it follows from (4.70) and (4.77) that $F_\xi(\zeta) = -\zeta^3/3 + \xi\zeta + r_n(\zeta)$, where $|r_n(\zeta)| \leq C\delta_n^{2/3}$. Also

$$\alpha\left|\frac{a+z_c}{(a+z_c+\gamma\omega n^{-1/3})}-1\right| \leq C/a^2, \tag{4.80}$$

if $\omega \in \mathcal{D}_1+\bar{\mathcal{D}}_1$ and thus we can approximate $\tilde{M}_n^{(1)}(\xi,\eta)$ with

$$\frac{\alpha}{(2\pi i)^2}\int_{\mathcal{C}_1+\bar{\mathcal{C}_1}} d\zeta \int_{\mathcal{D}_1+\bar{\mathcal{D}}_1} d\omega e^{-\zeta^3/3+\xi\zeta+\omega/3-\eta\omega}\frac{1}{\omega-\zeta} \tag{4.81}$$

Note that, if $|\zeta| \geq n^{1/15}$, then $\xi/|\zeta|^2 \leq Ca^{4/3}/n^{2/15} \leq C\delta_n^{4/3}$ and thus, with a negligible error, we can replace the expression in (4.81) by $\alpha K_{\mathrm{Ai}}(\xi,\eta)$. This completes the proof of the claim and the theorem. □

We can now prove Theorem 2.8.

Proof of Theorem 2.8. We show that the entries of the inverse Kasteleyn matrix under the rescaling given in the theorem converge to the entries of the inverse Kasteleyn matrix given in (2.20). By using Theorem 2.2, we can conclude that the two measures agree on cylinder sets.

Without loss of generality, we assume that $x_1 < y_1 + 1$ which means that $K^{-1}(x, y) = f_1(x, y)$ for $x = (x_1, x_2)$ and $y = (y_1, y_2)$. Let

$$g_{\alpha_1,\alpha_2}(z) = \alpha_2 \log(a + z) + (1 - \alpha_2) \log(az - 1) - \alpha_1 \log z \tag{4.82}$$

We have that $g'_{\alpha_1,\alpha_2}(z) = 0$ for z equal to

$$\frac{a^2\alpha_1 - \alpha_1 + \alpha_2 + a^2\alpha_2 - a^2 \pm \sqrt{-4a^2(1-\alpha_1)\alpha_1 + (\alpha_2 - \alpha_1 + a^2(\alpha_2 + \alpha_1 - 1))^2}}{2a(1-\alpha_2)}. \tag{4.83}$$

Suppose that z_c is the positive square root of the above equation. The square root term of z_c is given by

$$\begin{aligned} &- 4a^2(1-\alpha_1)\alpha_1 + (\alpha_2 - \alpha_1 + a^2(\alpha_2 + \alpha_1 - 1))^2 \\ &= \left(\frac{(\alpha_1 - \alpha_2)^2}{a^2} + (\alpha_2 + \alpha_1 - 1)^2 \right) a^2(1 + a^2) - a^2 \end{aligned} \tag{4.84}$$

which is less than zero for $\alpha_1, \alpha_2 \in \mathcal{D}$. This means that z_c is complex for α_1 and α_2 in the interior unfrozen region. By a computation, we have that

$$|z_c| = \sqrt{\frac{\alpha_1}{1 - \alpha_1}} =: r_1. \tag{4.85}$$

We also have

$$\left| \frac{a + z_c}{az_c - 1} \right| = \sqrt{\frac{\alpha_2}{1 - \alpha_2}} =: r_2. \tag{4.86}$$

We choose $x = (x_1, x_2)$ and $y = (y_1, y_2)$ as given in the theorem. As the double contour integrals are standard and the techniques of steepest descent are very well-established for this type of double contour integral formula, we omit the technical computational details for providing the bounds of the error terms. For $f_1(x, y)$, the contour $\mathcal{E}_1$ can be deformed to a contour from $\overline{z_c}$ to z_c and a contour from z_c to $\overline{z_c}$ which passes to the left of the origin. The contour $\mathcal{E}_2$ can be deformed to a contour which passes to the left of $1/a$ but also passes through the points $\overline{z_c}$ and z_c. This deformation picks up a single integral obtained from setting $z = w$ in the expression from $f_1(x, y)$ while the remaining double integrals can be shown to be $O(n^{-1/2})$ see [33] for example. We find that $f_1(x, y)$ is given by

$$\frac{i(-1)^{(\xi_1+\xi_2+\eta_1+\eta_2)/2}}{2\pi i} \int_{\overline{z_c}}^{z_c} z^{\eta_1 - \xi_1 - 1} \frac{1}{a + z} \left(\frac{a + z}{az - 1} \right) z^{\xi_2 - \eta_2} dz + O(n^{-1/2}). \tag{4.87}$$

We can make the change of variables $w = (a + z)/(az - 1)$. We find that $f_1(x, y)$ is now given by

$$\frac{i(-1)^{(\xi_1+\xi_2+\eta_1+\eta_2)/2}}{2\pi i} \int_{t(\overline{z_c})}^{t(z_c)} \left(\frac{a + w}{aw - 1} \right)^{\xi_1 - \eta_1 - 1} \frac{w^{\eta_2 - \xi_2 - 1}}{aw - 1} dw + O(n^{-1/2}) \tag{4.88}$$

where $t(z) = (a + z)/(az - 1)$. The above integral converges uniformly to

$$\frac{i(-1)^{(\xi_1+\xi_2+\eta_1+\eta_2)/2}}{(2\pi i)^2} \int_{|w|=r_2} \int_{|z|=r_1} \frac{z^{\eta_1 - \xi_1} w^{\eta_2 - \xi_2}}{a + w + z - awz} dz\, dw. \tag{4.89}$$

for $\xi_1, \xi_2, \eta_1, \eta_2 \in \mathbb{Z}$. This is due to $|a+w|/|aw-1| \leq r_1$ if and only if $w \in [t(\overline{z_c}), t(z_c)]$ and so one can use the residue formula to obtain (4.88) from (4.89). We can take the change of variables $z \mapsto z\alpha_1/i$ and $w \mapsto w\alpha_2/i$ in (4.89) and we obtain

$$r_1^{\eta_1-\xi_1-1} r_2^{\eta_2-\xi_2-1} \frac{(-1)^{\eta_1+\eta_2+1}}{(2\pi i)^2} \int_{|w|=1} \int_{|z|=1} \frac{z^{\eta_1-\xi_1} w^{\eta_2-\xi_2}}{P(zr_1, Pr_2)} \frac{dz}{z} \frac{dw}{w}. \tag{4.90}$$

Computing the probability of any cylinder set using the inverse Kasteleyn matrix given by (2.20) agrees with using the inverse Kasteleyn matrix given by (4.90) provided that $e^{B_x} = r_1$ and $e^{B_y} = r_2$.

□

5. Gaussian Free Field

In this section, we continue our study of the asymptotics of domino tilings of the Aztec diamond. We introduce the required complex structure for Theorem 2.9. We compute the necessary asymptotics of the inverse Kasteleyn entries and use them to prove Theorem 2.9. The approach of the proof closely mirrors [3] and [35] but uses the determinantal process obtained from the inverse Kasteleyn matrix in the spirit of [27]. This is due to the height function of domino tilings of the Aztec diamond uses dominos as opposed to the interlaced particle system. To compute the asymptotics of the inverse Kasteleyn matrix in the bulk, we follow the approach given in [12] which computes the asymptotics of a similar double contour integral. As the proof showing that the height fluctuations is well-established by the methods from [3], we do not provide all the technical details of the proof – we refer the reader to [3] and [35] where the same type of estimates have been computed for lozenge tilings.

5.1. Complex Structure.

In this subsection, we introduce the complex structure as well as the notation that is required for the rest of the section. Define $g : \mathbb{H} \to \mathbb{C}$ by

$$g(z|(x_1, x_2)) = x_2 \log(a+z) + (1-x_2)\log(az-1) - x_1 \log z. \tag{5.1}$$

To every point (x_1, x_2), there exists at most one $\Omega \in \mathbb{H}$ such that $g'(\Omega|(x_1, x_2)) = 0$. If this map exists, we can define

$$\tilde{\mathcal{D}} = \{(x_1, x_2) | \Omega(x_1, x_2) \in \mathbb{H} \text{ exists } \} \tag{5.2}$$

We have the following the lemma for the map Ω which follows from a similar calculation in [12].

Lemma 5.1. *The map $(x_1, x_2) \mapsto \Omega(x_1, x_2)$ is a diffeomorphism from $\mathcal{D}$ to $\mathbb{H}$. Furthermore, we have $\mathcal{D} = \tilde{\mathcal{D}}$.*

Proof. Since $g'(\Omega) = 0$ where g is defined in (5.1), we can split the equation into its real and imaginary components which give

$$\begin{pmatrix} -\mathrm{Re}\frac{1}{\Omega} & \mathrm{Re}\left(\frac{1}{a+\Omega} - \frac{a}{a\Omega-1}\right) \\ -\mathrm{Im}\frac{1}{\Omega} & \mathrm{Im}\left(\frac{1}{a+\Omega} - \frac{a}{a\Omega-1}\right) \end{pmatrix} \begin{pmatrix} x_1 \\ x_2 \end{pmatrix} = \begin{pmatrix} -\mathrm{Re}\left(\frac{a}{a\Omega-1}\right) \\ -\mathrm{Im}\left(\frac{a}{a\Omega-1}\right) \end{pmatrix} \tag{5.3}$$

The determinant of the above matrix is equal to $a\mathrm{Im}(\Omega)/|\Omega|^2(1/|a+\Omega|^2 + 1/|a\Omega-1|^2)$ which is non-zero because $\Omega > 0$. Therefore, we have

$$\begin{pmatrix} x_1 \\ x_2 \end{pmatrix} = \begin{pmatrix} 1 - \frac{1}{1+|\Omega|^2} \\ \frac{|a+\Omega|^2}{(1+a^2)(1+|\Omega|^2)} \end{pmatrix} \tag{5.4}$$

The second statement of the proposition is a direct consequence of the fact that the largest contribution from each integral when computing $K^{-1}(x,y)$ for x and y in the liquid region, comes from saddle point analysis which requires $g'(z)=0$.

□

For the rest of this section, we use the notation for $f:\mathcal{D}\to\mathbb{R}$ that

$$\langle \phi, F\rangle := \int_{\mathcal{D}} \phi(x)F(x)dx. \tag{5.5}$$

where $\phi:\mathcal{D}\to\mathbb{R}$ is a compactly supported test function.

5.2. **Asymptotic Entries.** In this subsection, we compute the asymptotics of the inverse Kasteleyn matrix in the interior of the liquid region which is split into three lemmas computing the long range and short range asymptotic behavior for $f_1(x,y)$ and the asymptotic behavior for $f_2(x,y)$ for $x=(x_1,x_2)$ and $y=(y_1,y_2)$. We also state without proof three lemmas that compute the asymptotics of $f_1(x,y)$ where one or possibly both x and y are near to or on the edge. The proof of these lemmas are technical arguments that can be found by mirroring the analogous lemmas in [3] and [35].

In order to state the main lemma of this subsection, we first find the correct deformation of the contours for the function $g(z|(x_1,x_2))$. The function $g(z|(x_1,x_2))$ has saddle points at the complex conjugates z_x and $\overline{z_x}$. We can deform the contour $\mathcal{E}_1$ into a closed counterclockwise oriented contour which passes through z_x and $\overline{z_x}$ and contains the origin. Label this contour Γ_1. We can deform the contour $\mathcal{E}_2$ into a contour which passes through z_x and $\overline{z_x}$ and is asymptotically parallel to the positive real axis. Label this contour Γ_2.

For the rest of the section, we drop the integer part from the computations. This has no effect on the computations.

Lemma 5.2. *For $X=(X_1,X_2), Y=(Y_1,Y_2)$ with $X,Y\in \mathrm{int}(n\mathcal{D})$ and $|X-Y|>n^{1/2+\delta}$ where $\delta>0$ then*

$$f_1(X,Y) = -\frac{1}{2\pi n}\sum_{\varepsilon_x,\varepsilon_y\in\{0,1\}} \frac{e^{n(g(z_x^{\varepsilon_x}|x)-g(z_y^{\varepsilon_y}|y))}}{(a+z_y^{\varepsilon_y})(z_x^{\varepsilon_x}-z_y^{\varepsilon_y})\sqrt{-g''(z_x^{\varepsilon_x})g''(z_y^{\varepsilon_y})}}\left(1+O(n^{-\delta/2}))\right) \tag{5.6}$$

where $X/n\to x=(x_1,x_2)$ and $Y/n\to y=(y_1,y_2)$ as $n\to\infty$, z_x solves $g'(z_x|x)=0$ with $\mathrm{Im}(z_x)>0$ and

$$z_x^{\varepsilon_x} = \begin{cases} z_x & \text{if } \varepsilon_x=0 \\ \overline{z_x} & \text{if } \varepsilon_x=1 \end{cases} \tag{5.7}$$

and respectively for y. We choose $\sqrt{-g''(z_x^0|x)}$ so that the orientation of the line $z=z_x+s/\sqrt{-g''(z_x^0|x)}$ is tangent to Γ_1 at z_x. We have a similar choice for $\sqrt{-g''(z_x^1|x)}$. We choose $\sqrt{g''(z_y^0|y)}$ so that the orientation of the line $z=z_y+t/\sqrt{g''(z_y^0|y)}$ is tangent to Γ_2 at z_y. We have a similar choice for $\sqrt{-g''(z_y^1|y)}$.

Proof. The argument for proving the lemma uses the steepest descent method following a very similar approach to [3, Proposition 6.9] and [12, Lemma 6.1].

Recall that we are computing the asymptotic behavior of

$$f_1(nx,ny) = \frac{1}{(2\pi i)^2}\int_{\mathcal{E}_1}\int_{\mathcal{E}_2}\frac{e^{n(g(z|x)-g(w|y)}}{(w+a)(w-z)}dzdw \tag{5.8}$$

where $nx = (nx_1, nx_2)$ and $ny = (ny_1, ny_2)$. The contributions to $f_1(nx, ny)$ come from each of the four pairs of saddle points. By the above choice of contours and the choice of the orientations of $g''(z_x^{\varepsilon_x}|x)$ and $g''(z_y^{\varepsilon_y}|y)$, we have the contributions outside of the four saddle points are exponentially small. Depending on the choice of x and y, we either have that $|z_x| \leq |z_y|$ or $|z_x| > |z_y|$. The restriction $|x - y| > n^{-1/2+\delta}$ imposes that $|z_x - z_y| > n^{-1/2+\delta}$. For $|z_x| \leq |z_y|$, the paths of steepest ascent and descent do not intersect.

In this calculation, we only consider the contribution pair (z_x, z_y) as the other three pairs follow from an analogous calculation. We introduce the change of variables

$$z = z_x + \frac{t}{\sqrt{-ng''(z_x)}} \tag{5.9}$$

and

$$w = z_y + \frac{s}{\sqrt{ng''(z_y)}}. \tag{5.10}$$

for $t, s \in [-n^{\delta/2}, n^{\delta/2}]$. We can expand the exponents in equation (5.8), namely, we have

$$ng(z) = ng(z_x) + \frac{ng''(z_x)}{2}(z - z_x)^2 + O(z - z_x)^3 = ng(z_x) - \frac{s^2}{2} + O(n^{-1/2+3\delta}) \tag{5.11}$$

and

$$ng(w) = ng(z_y) + \frac{ng''(z_y)}{2}(z - z_y)^2 + O(z - z_y)^3 = ng(z_y) + \frac{t^2}{2} + O(n^{-1/2+3\delta}). \tag{5.12}$$

Due to having $|z_x - z_y| > n^{-1/2+\delta}$, by continuity, we have that $|g''(z_x|x) - g''(z_y|y)| > n^{-1/2+\delta}$. We also have that $w + a = z_y + a + O(n^{-1/2})$ and $w - z = z_x - z_y + O(n^{-1/2})$. Therefore, uniformly on compact sets contained in $\mathrm{int}\mathcal{D}$, we have that the contribution from the saddle points z_x and z_y is given by

$$\frac{1}{(2\pi i)^2 n} \int_{-n^{\delta/2}}^{n^{\delta/2}} \int_{-n^{\delta/2}}^{n^{\delta/2}} \frac{e^{n(g(z_x|x) - g(z_y|y)) + (-s^2+t^2)/2}}{(z_y + a)(z_x - z_y)\sqrt{-g''(z_x|x)g''(z_y|y)}} ds dt + O(n^{-1/2+3\delta}) \tag{5.13}$$

By factoring out the constant terms, we can approximate the Gaussian integral which gives

$$-\frac{e^{n(g(z_x|x) - g(z_y|y))}}{2\pi n(z_y + a)(z_x - z_y)\sqrt{-g''(z_x|x)g''(z_y|y)}} + O(n^{-\delta/2}) \tag{5.14}$$

The other three contributions can be computed in exactly the same way.

For $|z_x| > |z_y|$, the contours Γ_1 and Γ_2 cross when applying the contour deformation to the paths of steepest ascent and descent. Due to the term $1/(w - z)$ in the integrand of $f_1(x, y)$, in addition to the double integral we obtain an extra term

$$\frac{1}{2\pi i} \int_{\bar{\xi}}^{\xi} \frac{e^{n(g(z|x) - g(z|y)}}{z + a} dz \tag{5.15}$$

where ξ denotes the intersection of the deformation of the two contours Γ_1 and Γ_2 onto their paths of steepest descent and ascent. The double integral term can be computed asymptotically as given in the case $|z_x| \leq |z_y|$ and the same expression holds. For the single integral given in (5.15), we wish to bound the integral and show that it is negligible. Manipulating g, we have that

$$\mathrm{Re}(g(z|x) - g(z|y)) = (y_1 - x_1)\log|z| - (y_2 - x_2)\log\left|\frac{az - 1}{a + z}\right| < 0 \tag{5.16}$$

for $0 < \arg(z) < \pi/2$ because $|(az-1)/(a+z)| < 1$. We can choose a contour from $\overline{\xi}$ to ξ so that $\mathrm{Re}z < \mathrm{Re}\xi$, which gives

$$e^{n\mathrm{Re}(g(z|x)-g(z|y))} \leq e^{n\mathrm{Re}(g(\xi|x)-g(\xi|y))}. \tag{5.17}$$

As ξ lies on the contour of steepest ascent and descent, the right hand side decays exponentially with n. Therefore, we have

$$\left| \frac{1}{2\pi i} \int_{\overline{\xi}}^{\xi} \frac{e^{n(g(z|x)-g(z|y)}}{z+a} dz \right| \leq C \frac{e^{n\mathrm{Re}(g(\xi|x)-g(\xi|y))}}{\xi+a} \tag{5.18}$$

decays exponentially (compared to the asymptotics of the double integral).

□

The next lemma gives estimates for $f_1(X,Y)$ when X and Y are close but still in the interior.

Lemma 5.3. *For $X, Y \in \mathrm{int}(n\mathcal{D})$ with $|X-Y| \leq n^{1/2+\delta}$, we have*

$$|f_1(X,Y)| \leq C \frac{e^{n\mathrm{Re}(g(z_x|x)-g(z_y|y))}}{n^{1/2}} \tag{5.19}$$

where C is a constant and $X/n \to x$ and $Y/n \to y$ as $n \to \infty$.

Proof. The proof of this lemma follows an argument from [12, Lemma 6.2]. Similar to the proof of Lemma 5.2, we have to deform the contours to pass through their appropriate saddle points and split into the cases when $|z_x| > |z_y|$ and when $|z_x| \leq |z_y|$. The exponential decay of the extra single integral from the case $|z_x| > |z_y|$ holds from Lemma 5.2. It remains to bound the double integral, which is the same for $|z_x| > |z_y|$ and $|z_x| \leq |z_y|$, for each of the four pairs of saddle points. We only present the computation for the pair (z_x, z_y).

We apply the saddle point method from Lemma 5.2 using the same local co-ordinate transformation which gives the same Taylor expansions of $g(z|x)$ and $g(w|y)$. Contrary to Lemma 5.2, we have that

$$z - w = z_x - z_y + \frac{s}{\sqrt{-g''(z_x|x)n}} + \frac{t}{\sqrt{-g''(z_y|y)n}} + O\left(n^{-1}\right). \tag{5.20}$$

where $|z_x - z_y| \leq n^{\delta-1/2}$. By continuity, we have that $g''(z_y|y) - g''(z_x|x)$ is $O(n^{-1/2+\delta})$. Either $|z_x - z_y| < n^{-1/2}$ or $|z_x - z_y|$ is of order $n^{-1/2+\alpha}$ for $0 \leq \alpha \leq \delta$, which means that we either choose $z_x - z_y$ or $\frac{s}{\sqrt{-g''(z_x|x)n}} + \frac{t}{\sqrt{-g''(z_y|y)n}}$ when estimating $z - w$. In any case, after bounding the integral we obtain a Gaussian integral which can be estimated to give the result. □

The next lemma finds bounds for $f_2(X,Y)$ which holds for all values of X and Y in the bulk and near the edge.

Lemma 5.4. *For $X = (X_1, X_2), Y = (Y_1, Y_2)$ with $X, Y \in n\mathcal{D}$, we have*

$$|f_2(X,Y)| \leq C \frac{e^{n\mathrm{Re}(\tilde{g}(z_c))}}{\sqrt{n}} \tag{5.21}$$

where C is a constant,

$$\tilde{g}(z) = (y_2 - x_2)\left(\log(az-1) - \log(a+z)\right) + (y_1 - x_1)\log z, \tag{5.22}$$

z_c is chosen so that $g'(z_c) = 0$ with $z_c \in \mathbb{H}$ and $X/n \to x$ and $Y/n \to y$ as $n \to \infty$.

Proof. By performing the change of variables $z \mapsto z - 1/a$, we can rewrite the integral so that the contour of integration is around the origin. The upper bound follows by using a one-dimensional steepest descent argument around z_c and $\overline{z_c}$.

□

The following lemmas consider the behavior of f_1 near or at the edge and finds bounds to limit the behavior. In order to state these lemmas, we distinguish the three regimes as in [3, 35]:

$$\begin{array}{ll} \inf_{x\in\partial\mathcal{D}} |X - xn| > n^{2/3} & (X \text{ is in the liquid region}) \\ cn^{1/3} < \inf_{x\in\partial\mathcal{D}} |X - xn| \leq n^{2/3} & (X \text{ is close to the edge}) \\ \inf_{x\in\partial\mathcal{D}} |X - xn| \leq cn^{1/3} & (X \text{ is at the edge}) \end{array} \tag{5.23}$$

We do not include the proofs of these technical lemmas because they involve estimates of the double and single contour integrals f_1 and f_2 which follow from very similar computations given in both [3, Proposition 6.11-6.13] and [35, Lemma 4.15-4.17].

Lemma 5.5. *For $X, Y \in \text{int}(n\mathcal{D})$ with $X/n \to x$ and $Y/n \to y$, with one or both $x = (x_1, x_2)$ and $y = (y_1, y_2)$ in $\partial\mathcal{D}$ and assume that $|z_x - z_y|$ is uniformly bounded away from zero in n. Then, we have*

$$|K^{-1}(X, Y)| \leq C \frac{e^{n\text{Re}(g(z_x|x) - g(z_y|x))}}{n\sqrt{g''(z_x|x)g''(z_y|y)}} \tag{5.24}$$

uniformly in n where C is a constant.

Lemma 5.6. *Suppose that $X \in n\mathcal{D}$ is close to the edge and $Y \in \text{int}(n\mathcal{D})$ and $X/n \to x = (x_1, x_2) \in \partial\mathcal{D}$ and $Y \to y = (y_1, y_2) \in \text{int}(\mathcal{D})$. Then, we have*

$$|K^{-1}(X, Y)| \leq C \frac{e^{n\text{Re}(g(z_x) - g(z_y)) + n^{1/3} g(z_x|X - x/n)}}{n^{\frac{5}{6}}\sqrt{g''(z_y|y)}} \tag{5.25}$$

uniformly in n where C is a constant.

It can be shown that $n^{1/3} g(z_x|X - x/n)$ is order $n^{2/3}$ and is negative.

Lemma 5.7. *Suppose that $X, Y \in n\mathcal{D}$ are on the edge with $X \to x \in \partial\mathcal{D}$ and $Y \to y \in \partial\mathcal{D}$ and that $|z_x - z_y|$ is bounded away from 0 uniformly in n. Then, we have*

$$|K^{-1}(X, Y)| \leq C \frac{e^{n\text{Re}(g(z_x) - g(z_y)) + n^{1/3} g(z_x|X - x/n) + n^{1/3} g(z_y|Y - y/n)}}{n^{\frac{2}{3}}} \tag{5.26}$$

uniformly in n where C is a constant.

5.3. **Proof of Theoem 2.9.** Before proving Theorem 2.9, we introduce some notation. Let $\mathcal{D}_n$ denote the unfrozen region of A_n with lattice space $1/n$. Let $\mathcal{H}_n^{m,\delta}$ be the set

$$\{(x_1, \ldots, x_m) \in \text{int}(\mathcal{D}_n^m) : \exists i, j \text{ such that } |x_i - x_j| \leq n^{-1/2+\delta}\} \tag{5.27}$$

Proof of Theorem 2.9. The aim is to show that we can write the moments of the pushforward of h under the map Ω as a Gaussian with covariance given (2.23). For tiling models with frozen and unfrozen regions, this approach was first considered in [3] and later used in a universal setting in [35]. We follow the outline of these approaches and refer the reader to these papers for the full technical details.

For $x \in \mathcal{D}_n$, let $\tilde{h}_n = h_n(\Omega^{-1}(x))$, where n is the size of A_n and h_n is the height function of the Aztec diamond of size n. Let $\tilde{h}_n^a$ denote the average height of $\tilde{h}_n$ and let $\tilde{H}_n = \tilde{h}_n - \tilde{h}_n^a$.

Similarly, let h_n^a denote the average height of h_n, and $H_n = h_n - h_n^a$. For compactly supported continuous test functions $\phi_i \in C_c(\mathbb{R}^2)$, we have

$$\mathbb{E}\left[\prod_{i=1}^{m}\left\langle \tilde{H}_n, \phi_i\right\rangle\right] = \mathbb{E}\int_{\mathcal{D}_n^m}\prod_{i=1}^{m}\phi_i(x_i)\tilde{H}_n(x_i)|dx_1|^2\cdots|dx_m|^2, \tag{5.28}$$

where the integral is the Riemann sum over the faces of $\mathcal{D}_n$, that is,

$$\left\langle \tilde{H}_n, \phi\right\rangle = \int_{\mathcal{D}_n}\tilde{H}_n(x)\phi(x)|dx|^2 = \frac{1}{n^2}\sum_{\substack{x \text{ face}\\ \text{in D}}}\tilde{H}_n(x)\phi(x).$$

In order to estimate $\mathbb{E}[\prod_{i=1}^m \tilde{H}_n(x_i)]$, we will first estimate $\mathbb{E}[\prod_{i=1}^m H_n(x_i)]$. Using the definition of the height function (2.13), we have the following: suppose $\gamma_1, \ldots, \gamma_m$ are paths from distinct points on the boundary to $x_1, \ldots, x_m$, where we assume that $|x_i - x_j| > n^{-1/2+\delta}$, we have

$$\mathbb{E}\left[\prod_{i=1}^{m}H(x_i)\right] = \sum_{\substack{i\in\gamma_1\\ \vdots\\ i_m\in\gamma_m}}\mathbb{E}\left[(X_{i_1}-\mathbb{E}\left[X_{i_1}\right])\cdots(X_{i_m}-\mathbb{E}\left[X_{i_m}\right])\right](-1)^{i_1+\cdots+i_m}3^m \tag{5.29}$$

where $i_j \in \gamma_j$ denotes the i_j^{th} index of the curve γ_j.

The above summand can be computed explicitly using the local statistics formula (2.6) and the corresponding formulas in [26]. The summand (5.29) gives

$$(-1)^{i_1+\cdots+i_m}3^m\prod_{j=1}^{m}K(w_{i_1},b_{i_1}) \det\begin{vmatrix} 0 & K^{-1}(b_{i_2},w_{i_1}) & \cdots & K^{-1}(b_{i_m},w_{i_1})\\ K^{-1}(b_{i_1},w_{i_2}) & & & \\ \vdots & \ddots & \ddots & \vdots \\ & & & K^{-1}(b_{i_m},w_{i_{m-1}})\\ K^{-1}(b_{i_1},w_{i_m}) & \cdots & K^{-1}(b_{i_{m-1}},w_{i_m}) & 0\end{vmatrix}, \tag{5.30}$$

where b_{i_j} and w_{i_j} are the black and white vertices crossed by γ_j. As we have chosen $|x_i - x_j| > n^{-1/2+\delta}$, i.e. $(x_1, \ldots, x_n) \in \mathcal{D}_n^m \setminus \mathcal{H}_{n,\delta}^m$, we can write (5.30) using Lemmas 5.2 to 5.4, up to highest order. Without loss of generality, assume that all γ_i's only cross horizontal edges, and assume that the edges are of the form (W_0, B_0) or (B_1, W_1). Therefore, using the multilinearity of the determinant and the above discussion on the entries, we have that the highest order term is equal to

$$\sum_{\epsilon_1,\ldots,\epsilon_m\in\{0,1\}}\frac{3^m(-1)^{\epsilon_1+\ldots+\epsilon_m}}{(2\pi)^m\prod_{j=1}^m g''(z_j^{\epsilon_j})}\det\begin{bmatrix}0 & \frac{e^{n(g(z_2^{\epsilon_2})-g(z_1^{\epsilon_1}))}}{z_2^{\epsilon_2}-z_1^{\epsilon_1}} & \cdots & \frac{e^{n(g(z_n^{\epsilon_n})-g(z_1^{\epsilon_1}))}}{z_n^{\epsilon_n}-z_1^{\epsilon_1}}\\ & & \ddots & \vdots \\ & & & 0\end{bmatrix}, \tag{5.31}$$

where $z_j^{\epsilon_j} = z_{x_j}^{\epsilon_j}$ and x_j is the coordinate of b_j, which is defined in Lemma 5.2.

One of the expansions of the above determinant gives

$$\sum_{\sigma} \operatorname{sgn}(\sigma) \sum_{\epsilon_1,\dots,\epsilon_n \in \{0,1\}} 3^m \frac{(-1)^{\epsilon_1+\cdots+\epsilon_m}}{2\pi^m \prod_{j=1}^m g''(z_j^{\epsilon_j})} \prod_{j=1}^m \frac{1}{z_j^{\epsilon_j} - z_{\sigma_j}^{\epsilon_{\sigma_k}}}. \tag{5.32}$$

whereas the rest of the expansion gives a term, which we will call $G(z)$ which contains the oscillatory parts of (5.31). We can find $G(z)$ by subtracting (5.31) by (5.32)

Therefore, we have an expression of $\mathbb{E}[\prod H(x_i)]$ and moreover, we have an expression of $\mathbb{E}[\prod \tilde{H}(x_i)]$. Using the convergence of the Riemann sum and writing

$$dz_i^{\epsilon_i} \approx \frac{1}{3g''(\Omega(z_i^{\epsilon_i}))} \frac{1}{n}$$

for the map $z_i \mapsto \Omega(z_i)$, we have

$$\begin{aligned} \mathbb{E}\left[\prod_{i=1}^m \tilde{H}(x_i)\right] &= \sum_{\sigma \in S_n} \operatorname{sgn}(\sigma) \sum_{\epsilon_1,\dots,\epsilon_n \in [0,1]} (-1)^{\epsilon_1+\cdots+\epsilon_n} \frac{1}{(2\pi)^m} \\ &\quad \times \int_{\Omega(\gamma_1)} \cdots \int_{\Omega(\gamma_m)} \prod_{j=1}^m \frac{1}{z_{\sigma_j}^{\epsilon_{\sigma_j}} - z_{\sigma_{j-1}}^{\epsilon_{\sigma_{j-1}}}} dz_1^{\epsilon_1} \cdots dz_m^{\epsilon_m} + O(n^{-1}). \end{aligned} \tag{5.33}$$

by using the Riemann Lebesgue theorem which gives the integrals containing $G(z)$ converge to zero as n tends to infinity.

Using [5, Lemma 7], which says that

$$\sum_{\sigma \in m-\text{cycle}} \prod_{i=1}^m \frac{1}{z_{\sigma_i} - z_{\sigma_{i-1}}} = 0, \tag{5.34}$$

we have that the only terms remaining from (5.33) are the fixed point free involutions. We obtain

$$\mathbb{E}\left[\prod_{i=1}^m \tilde{H}(x_i)\right] = \sum_{\text{pairings } \sigma} \prod_{i=1}^{m/2} \tilde{G}(\Omega(x_{\sigma_i}), \Omega(x_{\sigma_{i+1}}))$$

where $\tilde{G}$ will be found when we compute the variance.

There are two technical considerations for $\mathbb{E}\left[\prod_{i=1}^m \tilde{H}(x_i)\right]$ – one where some of the points x_i are near to the edge and the second when some of the points x_i are close together, i.e. $x_i \in \mathcal{H}_{n,\delta}^m$. In either case, we outline the main points of the argument. For a full technical proof of these considerations, one can mirror the approach in [3] or [35].

For the case where some of the x_i's are close to the edge, one can approximate $\mathbb{E}\left[\prod_{i=1}^m \tilde{H}(x_i)\right]$ using the computation given above in the following way: as we are free to choose the paths γ_i and their boundary end points, we make the choice so that the boundary endpoints of each γ_i are closest to x_i if x_i is close or on the edge. For example, if nx_i is $n^{1/2}$ from the edge, then the path length of γ_i (before rescaling) is order $n^{1/2}$. Using the estimates in Lemma 5.5- 5.7 and the appropriate choice of each γ_i, then the approximation of $\mathbb{E}\left[\prod_{i=1}^m \tilde{H}(x_i)\right]$ using the Riemann sum as above will tend to zero (due to summing over too fewer points).

When some of the x_i's are in $\mathcal{H}_{n,\delta}^m$, we can approximate the $\mathbb{E}\left[\prod_{i=1}^m \tilde{H}(x_i)\right]$ by first considering all the x_i's not in $\mathcal{H}_{n,\delta}^m$ using the approach given above and then add an approximation in the neighborhood of x_i for x_i in $\mathcal{H}_{n,\delta}^m$. The latter approximation can be bounded

above by using Lemma 5.3 and Lemma 5.4. Thus, one is able to have an upper bound of $\mathbb{E}\left[\prod_{i=1}^{m}\tilde{H}(x_i)\right]$ by n^{ϵ} where $\epsilon > 0$. More formal versions of this argument can be found in [3, 27, 35]. A consequence of this argument is that integrating $\mathbb{E}\left[\prod_{i=1}^{m}\tilde{H}(x_i)\right]$ over $\mathcal{H}_{n,\delta}^{m}$ tends to zero as n tends to ∞. That is,

$$\lim_{n\to\infty}\mathbb{E}\int_{\mathcal{H}_{n,\delta}^{m}}\prod_{i=1}^{m}\phi_i(x_i)\tilde{H}_n(x_i)|dx_1|^2\cdots|dx_m|^2 = 0. \tag{5.35}$$

Finally, we have

$$\begin{aligned}\lim_{n\to\infty}\mathbb{E}\left[\prod_{i=1}^{m}\left\langle\tilde{H}_n,\phi_i\right\rangle\right] &= \lim_{n\to\infty}\int_{\mathcal{D}_n^m\setminus\mathcal{H}_n^m}\cdots + \int_{\mathcal{H}_n^m}\cdots \\ &= \lim_{n\to\infty}\int_{\mathcal{D}_n^m\setminus\mathcal{H}_n^m}\cdots \\ &= \sum_{\text{pairings}}\int_{\mathcal{D}_n^m}\prod_{i=1}^{m}\phi(x_i)\prod_{i=1}^{m/2}\tilde{G}(x_{\sigma(i)},x_{\sigma(i+1)})|dx_1|^2\cdots|dx_n|^2.\end{aligned}$$

where $\cdots$ represents the integrand given in equation (5.28). It remains to compute the variance. Using Equation (5.33), we have that

$$\begin{aligned}\mathbb{E}\left[\prod_{i=1}^{m}\tilde{H}(x_i)\right] &= -\frac{1}{(2\pi)^2}\sum_{\epsilon_1,\epsilon_2}(-1)^{\epsilon_1+\epsilon_2}\int_{\Omega(\gamma_1)}\int_{\Omega(\gamma_2)}\frac{1}{(z_1-z_2)^2}dz_1^{\epsilon_1}dz_2^{\epsilon_2} \\ &= -\frac{1}{(2\pi)^2}\ln\left|\frac{\Omega(x_1)-\Omega(x_2)}{\Omega(x_1)-\overline{\Omega(x_2)}}\right| \\ &= \frac{1}{2\pi}G(\Omega(x_1),\Omega(x_2)).\end{aligned}$$

This means that $\tilde{G} = G_r$ as required.

□

6. Dimers to Particles: Guessing K^{-1}

It is easy to derive a correlation kernel for the zig-zag particle point process in the Aztec diamond from the knowledge of the inverse Kasteleyn kernel using Theorem 2.3. The transformation between the coordinate system used in [19] for the particles (u_1, u_2) and the coordinate system (x_1, x_2) used for the dimers in this paper is

$$\begin{cases} u_1 = x_2 \\ u_2 = (x_2 - x_1 + 1)/2. \end{cases} \tag{6.1}$$

The correlation kernel for the zig-zag particles is given by [19]

$$K_n(u_1,u_2;v_1,v_2) = \tilde{K}_n(u_1,u_2;v_1,v_2) - \phi_{u_1,v_1}(u_2,v_2) \tag{6.2}$$

where

(6.3)

$$\tilde{K}_n(2r-\varepsilon_1,u_2;2s-\varepsilon_2,v_2) = \frac{1}{(2\pi i)^2}\int_{\gamma_{r_1}}\frac{dw}{w}\int_{\gamma_{r_2}}\frac{dz}{z}\frac{z^{v_2}}{w^{u_2}}\frac{(1-az)^{n-s+\varepsilon_2}(1+a/z)^s}{(1-aw)^{n-r+\varepsilon_1}(1+a/w)^r}\frac{w}{w-z},$$

$$\phi_{2r-\varepsilon_1,2s-\varepsilon_2}(u_2,v_2) = \frac{\mathbb{1}(2r-\varepsilon_1<2s-\varepsilon_2)}{2\pi i}\int_{\gamma_1} z^{v_2-u_2}\frac{(1-az)^{r-s+\varepsilon_2-\varepsilon_1}}{(1+a/z)^{r-s}}\frac{dz}{z} \tag{6.4}$$

and $\varepsilon_1,\varepsilon_2\in\{0,1\}$, $a<r_1<1/a$, $0<r_2<r_1$.

Note that we have a zig-zag particle at $b\in\mathtt{B}$ if and only if a dimer covers the edge $(b-e_1,b)$ or the edge $(b-e_j,b)$. Thus, for $b_1,b_2\in\mathtt{B}$ it follows from Theorem 2.3 that

$$\begin{aligned}\mathbb{P}[\text{particles at } b_1 \text{ and } b_2] &= \sum_{r_1,r_2=1}^{2} K(b_1,b_1-e_{r_1})K(b_2,b_2-e_{r_2})\det(K^{-1}(b_i-e_{r_i},b_j))_{i,j=1,2}\\ &= \det\left(\sum_{r=1}^{2} K(b_i,b_i-e_r)K^{-1}(b_i-e_r,b_j)\right)_{i,j=1,2}\end{aligned} \tag{6.5}$$

Let b_1 have particle coordinates (u_1,u_2) and dimer coordinates (x_1,x_2) and let b_2 have particle coordinates (v_1,v_2) and dimer coordinates (y_1,y_2). We also have

$$\mathbb{P}[\text{particles at } b_1 \text{ and } b_2] = \det\begin{pmatrix} K_n(u_1,u_2;u_1,u_2) & K_n(v_1,v_2;u_1,u_2)\\ K_n(u_1,u_2;v_1,v_2) & K_n(v_1,v_2;v_1,v_2)\end{pmatrix} \tag{6.6}$$

(or the transpose of the same matrix).

It is not obvious how to make an identification between the elements in the determinants in (6.5) and (6.6), but it reasonable that something like

$$\frac{\psi(v_1,v_2)}{\psi(u_1,u_2)}K_n(v_1,v_2;u_1,u_2) = K(b_1,b_1-e_1)K^{-1}(b_1-e_1,b_2)+K(b_1,b_1-e_2)K^{-1}(b_1-e_2,b_2) \tag{6.7}$$

could hold with an appropriate ψ. Inserting the coordinates and using (6.1) we get

$$\begin{aligned}&\frac{\tilde\psi(y_1,y_2)}{\tilde\psi(x_1,x_2)}K_n\left(y_2,\frac{y_2-y_1+1}{2};x_2,\frac{x_2-x_1+1}{2}\right)\\ &= -(-1)^{-(x_1+x_2-1)/2}\left(K^{-1}((x_1-1,x_2-1),(y_1,y_2))-aiK^{-1}((x_1+1,x_2-1),(y_1,y_2))\right)\end{aligned} \tag{6.8}$$

Note that for the zig-zag particles on the black vertices, we have $x_1\in2\mathbb{Z}$ and $x_2\in2\mathbb{Z}+1$. Hence, we can write $u_1=x_2=2s-1$, $v_1=y_2=2r-1$, i.e. $r=(y_2+1)/2$, $s=(x_2+1)/2$. It follows from (6.3) that

$$\begin{aligned}&\tilde K_n\left(y_2,\frac{y_2-y_1+1}{2};x_2,\frac{x_2-x_1+1}{2}\right)\\ &= \frac{(-1)^{(y_2-x_2)/2}}{(2\pi i)^2}\int_{\gamma_{r_1}}dw\int_{\gamma_{r_2}}dz\frac{w^{y_1/2}}{z^{x_1/2}}\frac{(az-1)^{n-(x_2+1)/2+1}(z+a)^{(x_2+1)/2}}{(aw-1)^{n-(y_2+1)/2+1}(w+a)^{(y_2+1)/2}}\frac{1}{z(w-z)}\end{aligned} \tag{6.9}$$

We now use the identity

$$\frac{z+a}{z^{x_1/2}} = (-1)^{-(x_1+x_2-1)/2}(-1)^{(x_1+x_2)/4-(y_1+y_2)/4}\begin{bmatrix}\dfrac{(-1)^{(x_1-1+x_2-1+y_1+y_2)/4}}{z^{(x_1-1-1)/2}}\\ -ai\dfrac{(-1)^{(x_1+1+x_2-1+y_1+y_2)/4}}{z^{(x_1+1-1)/2}}\end{bmatrix} \tag{6.10}$$

in (6.9). Note that we have

$$(-1)^{(y_2-x_2)/2}(-1)^{(x_1+x_2)/4-(y_1+y_2)/4} = (-1)^{(x_1-x_2)/4-(y_1-y_2)/4}. \tag{6.11}$$

Choose $\tilde{\psi}(x_1, x_2) = (-1)^{(x_2-x_1)/4}$ in (6.8). We then get using (6.10) in (6.9)

$$-\frac{\tilde{\psi}(y_1,y_2)}{\tilde{\psi}(x_1,x_2)}\tilde{K}_n\left(y_2, \frac{y_2-y_1+1}{2}; x_2, \frac{x_2-x_1+1}{2}\right) \tag{6.12}$$

$$= (-1)^{-(x_1+x_2-1)/2}\left(f_1((x_1-1,x_2-1),(y_1,y_2)) - aif_1((x_1+1,x_2-1),(y_1,y_2))\right), \tag{6.13}$$

where f_1 is given by (2.26). If we similarly write

$$-\frac{\tilde{\psi}(y_1,y_2)}{\tilde{\psi}(x_1,x_2)}\left(\phi_{y_2,x_2}\left(\frac{y_2-y_1+1}{2}, \frac{x_2-x_1+1}{2}\right)\right)$$

$$= (-1)^{-(x_1+x_2-1)/2}\left(f_2((x_1-1,x_2-1),(y_1,y_2)) - aif_2((x_2+1,x_2-1),(y_1,y_2))\right) \tag{6.14}$$

using (6.4), (6.10) and (6.11) we get

(6.15)

$$f_2((x_1,x_2),(y_1,y_2)) = -\frac{(-1)^{(x_1+x_2+y_1+y_2)/4}}{2\pi i}\mathbb{1}(y_2<x_2)\int_{\gamma_1} z^{(y_1-x_1+1)/2)}\frac{(az-1)^{(y_2-x_2-1)/2}}{(z+a)^{(y_2-x_2+1)/2}}\frac{dz}{z}.$$

That this is the same as the $f_2((x_1, x_2), (y_1, y_2))$ defined by (2.28) follows from the following computation:

$$\begin{aligned}
&\mathbb{1}(y_2<x_2)\int_{\gamma_1} z^{(y_1-x_1+1)/2)}\frac{(az-1)^{(y_2-x_2-1)/2}}{(z+a)^{(y_2-x_2+1)/2}}\frac{dz}{z}\\
&= \mathbb{1}(y_2<x_2)\mathbb{1}(y_1<x_1)\int_{\gamma_1} z^{(y_1-x_1+1)/2)}\frac{(az-1)^{(y_2-x_2-1)/2}}{(z+a)^{(y_2-x_2+1)/2}}\frac{dz}{z}\\
&= -\mathbb{1}(y_2<x_2)\mathbb{1}(y_1<x_1)\int_{|z-1/a|=\varepsilon} z^{(y_1-x_1+1)/2)}\frac{(az-1)^{(y_2-x_2-1)/2}}{(z+a)^{(y_2-x_2+1)/2}}\frac{dz}{z}\\
&= -\mathbb{1}(y_1<x_1)\int_{|z-1/a|=\varepsilon} z^{(y_1-x_1+1)/2)}\frac{(az-1)^{(y_2-x_2-1)/2}}{(z+a)^{(y_2-x_2+1)/2}}\frac{dz}{z}\\
&= -\mathbb{1}(y_1<x_1)a^{(y_2-x_2-1)/2}\int_{|z|=\varepsilon}\frac{(z+1/a)^{(y_1-x_1-1)/2)}z^{(y_2-x_2-1)/2}}{(z+a+1/a)^{(y_2-x_2+1)/2}}dz.
\end{aligned}$$

If we combine (6.2), (6.8), (6.13) and (6.14) we are led to the conjecture

$$K^{-1}((x_1,x_2),(y_1,y_2)) = f_1((x_1,x_2),(y_1,y_2)) - f_2((x_1,x_2),(y_1,y_2)) \tag{6.16}$$

which is shown to be true in the proof of Theorem 2.3.

There is another approach based on looking instead at the probability of seeing a particle at a specified white vertex and a particle at a specified black vertex. This leads to the following relation between the particle kernel and the inverse Kasteleyn matrix,

(6.17)

$$K^{-1}((x_1,x_2),(y_1,y_2)) = -(-1)^{(x_1-x_2+y_1-y_2+2)/4}K_n(y_2, \frac{y_2-y_1+1}{2}; x_2, \frac{x_2-x_1+1}{2}),$$

where K_n is given by (6.2). Compare the relation found between the particle kernel and the inverse Kasteleyn matrix in [34].

References

[1] Greg W. Anderson, Alice Guionnet, and Ofer Zeitouni. *An introduction to random matrices*, volume 118 of *Cambridge Studies in Advanced Mathematics*. Cambridge University Press, Cambridge, 2010.

[2] Omer Angel, Alexander E. Holroyd, Dan Romik, and Bálint Virág. Random sorting networks. *Adv. Math.*, 215(2):839–868, 2007.

[3] A. Borodin and P. Ferrari. Anisotropic growth of random surfaces in 2+1 dimensions. arXiv:0804:3035, 2008.

[4] Alexei Borodin and Senya Shlosman. Gibbs ensembles of nonintersecting paths. *Comm. Math. Phys.*, 293(1):145–170, 2010.

[5] Cédric Boutillier. Pattern densities in non-frozen planar dimer models. *Comm. Math. Phys.*, 271(1):55–91, 2007.

[6] Cédric Boutillier and Béatrice de Tilière. The critical Z-invariant Ising model via dimers: the periodic case. *Probab. Theory Related Fields*, 147(3-4):379–413, 2010.

[7] Nathan Broomhead. Dimer models and Calabi-Yau algebras. *Mem. Amer. Math. Soc.*, 215(1011):viii+86, 2012.

[8] Henry Cohn, Noam Elkies, and James Propp. Local statistics for random domino tilings of the aztec diamond. *Duke Mathematical Journal*, 85(1):117–166, 1996.

[9] Henry Cohn, Richard Kenyon, and James Propp. A variational principle for domino tilings. *J. Amer. Math. Soc.*, 14(2):297–346 (electronic), 2001.

[10] B. de Tiliere. Conformal invariance of isoradial dimer models & the case of triangular quadri-tilings. *ANNALES DE L'INSTITUT HENRI POINCARÉ (B) PROBABILITÉS ET STA*, 43:729, 2007.

[11] J. Dubédat. Dimers and analytic torsion 1. arXiv:1110.2808, 2011.

[12] M. Duits. The gaussian free field in an interlacing particle system with two jump rates. arXiv:1105:4656, 2011.

[13] N. Elkies, G. Kuperberg, M. Larsen, and J. Propp. Alternating-sign matrices and domino tilings (part i). *Journal of Algebraic Combinatorics*, 1(2):111–132, 1992.

[14] Benjamin J. Fleming and Peter J. Forrester. Interlaced particle systems and tilings of the Aztec diamond. *J. Stat. Phys.*, 142(3):441–459, 2011.

[15] Israel Gohberg, Seymour Goldberg, and Nahum Krupnik. *Traces and determinants of linear operators*, volume 116 of *Operator Theory: Advances and Applications*. Birkhäuser Verlag, Basel, 2000.

[16] H. Helfgott. Edge effects on local statistics in lattice dimers: A study of the aztec diamond (finite case). *Arxiv preprint math/0007136*, 2000.

[17] W. Jockusch, J. Propp, and P. Shor. Random domino tilings and the arctic circle theorem. *Arxiv preprint math/9801068*, 1998.

[18] Kurt Johansson. Non-intersecting paths, random tilings and random matrices. *Probab. Theory Related Fields*, 123(2):225–280, 2002.

[19] Kurt Johansson. The arctic circle boundary and the Airy process. *Ann. Probab.*, 33(1):1–30, 2005.

[20] Kurt Johansson. Random matrices and determinantal processes. In *Mathematical statistical physics*, pages 1–55. Elsevier B. V., Amsterdam, 2006.

[21] Kurt Johansson and Eric Nordenstam. Eigenvalues of GUE minors. *Electron. J. Probab.*, 11:no. 50, 1342–1371, 2006.

[22] P. W. Kasteleyn. Graph theory and crystal physics. In *Graph Theory and Theoretical Physics*, pages 43–110. Academic Press, London, 1967.

[23] P.W. Kasteleyn. The statistics of dimers on a lattice: I. the number of dimer arrangements on a quadratic lattice. *Physica*, 27:1209–1225, 1961.

[24] Richard Kenyon. Local statistics of lattice dimers. *Ann. Inst. H. Poincaré Probab. Statist.*, 33(5):591–618, 1997.

[25] Richard Kenyon. Conformal invariance of domino tiling. *Ann. Probab.*, 28(2):759–795, 2000.

[26] Richard Kenyon. Dominos and the Gaussian free field. *Ann. Probab.*, 29(3):1128–1137, 2001.

[27] Richard Kenyon. Height fluctuations in the honeycomb dimer model. *Comm. Math. Phys.*, 281(3):675–709, 2008.

[28] Richard Kenyon. Lectures on dimers. In *Statistical mechanics*, volume 16 of *IAS/Park City Math. Ser.*, pages 191–230. Amer. Math. Soc., Providence, RI, 2009.

[29] Richard Kenyon, Andrei Okounkov, and Scott Sheffield. Dimers and amoebae. *Ann. of Math. (2)*, 163(3):1019–1056, 2006.

[30] L. S. Levitov. The rvb model as the problem of the surface of a quantum crystal. *JETP Letters*, 50(10):469–472, 1989.
[31] L. S. Levitov. Equivalence of the dimer resonance-valence-bond problem to the quantum roughening problem. *Phys. Rev. Lett.*, 64(1):92–94, 1990.
[32] Michael Luby, Dana Randall, and Alistair Sinclair. Markov chain algorithms for planar lattice structures. *SIAM J. Comput.*, 31(1):167–192 (electronic), 2001.
[33] Andrei Okounkov and Nikolai Reshetikhin. Correlation function of Schur process with application to local geometry of a random 3-dimensional Young diagram. *J. Amer. Math. Soc.*, 16(3):581–603 (electronic), 2003.
[34] Leonid Petrov. Asymptotics of random lozenge tilings via gelfand-tsetlin schemes. arXiv:1202.3901, 2012.
[35] Leonid Petrov. Asymptotics of uniformly random lozenge tilings of polygons. gaussian free field. arXiv:1206.5123, 2012.
[36] Scott Sheffield. Gaussian free fields for mathematicians. *Probab. Theory Related Fields*, 139(3-4):521–541, 2007.
[37] A. Soshnikov. Determinantal random point fields. *Uspekhi Mat. Nauk*, 55(5(335)):107–160, 2000.
[38] William P. Thurston. Conway's tiling groups. *Amer. Math. Monthly*, 97(8):757–773, 1990.